



WPI

Engineered Fibrotic Microenvironments with Heterogeneous Spatial Organization for *In Vitro* Disease Modeling

A Major Qualifying Project Report:

Submitted to the Faculty

of

Worcester Polytechnic Institute

In partial fulfillment of the requirements for the

Degree of Bachelor Science

By

David Chen

Yibin Chen

Kevin D'Agostino

Vu Nguyen

Advisors:

Professor Catherine Whittington, Ph.D

Date: May 18, 2020

Table of Contents

Table of Contents	1
Authorship	4
List of Figures	7
List of Tables	9
Acknowledgements	10
Abstract	11
1. Introduction	12
2. Literature Review	16
2.1 Fibrotic Phenomena	16
2.2 Pathophysiology of Fibrosis	17
2.2.1 Extracellular Matrix (ECM)	17
2.2.2 Tumor Microenvironment (TME)	19
2.3 Biomaterials used for In Vitro Tissue Models	20
2.3.1 Collagen	21
2.3.2 Gelatin	22
2.3.3 Alginate	24
2.3.4 Decellularized Matrix	24
2.4 Current Research	25
2.5 Matrix Modification Approaches	27
2.5.1 Microfluidic Spinning	28
2.5.2 Electrospinning	29
2.5.3 Macromolecular Crowding (MMC)	29
2.5.4 Bioprinting	31
3. Project Strategy	32
3.1 Client Statement	32
3.2 Design Requirements	32
3.2.1 Objectives	32
3.2.2 Constraints	35
3.2.3 Functions	36

3.3 Standards	37
3.4 Revised Client Statement	37
4. Design Process	39
4.1 Needs Analysis	39
4.1.1 ECM Manipulation Methods	39
4.1.2 ECM Materials	42
4.2 Alternative Designs	44
4.2.1 Single Agent Macromolecular Crowding	44
4.2.2 Mixed Agent Macromolecular Crowding	45
4.2.3 Electrospinning for 2.5D Scaffold Models and 3D Layering	46
4.2.4 Electrospun Layering within Hydrogel	47
4.3 Final Design Selection	48
5. Design Verification	51
5.1 Turbidity Assay with Macromolecular Crowders	51
5.2 MMC Confocal Imaging and Analysis	53
5.3 Electrospinning	58
6. Final Design Verification	61
6.1 Assessment of Objectives	61
6.1.1 Ease of Use	61
6.1.2 Heterogeneously Organized	61
6.1.3 In Vivo Characteristics	62
6.1.4 Reproducible	62
6.1.5 Cost Effective	63
6.2 Summary of Experimental Analysis	64
6.2.1 Means	64
6.2.2 Decellularization of Pancreas Tissue	65
6.2.3 Preparation of Collagen Hydrogel with Single Crowding Agents	66
6.2.3 Turbidity Analysis of Hydrogels with Single Crowders	66
6.2.4 MMC Confocal Imaging and Analysis	67
6.2.5 Preparation of Alginate/PEO with Electrospinning	68
6.3 Impact of Final design	69
6.3.1 Economics	69
6.3.2 Environmental Impact	69
6.3.3 Societal Impact	70
6.3.4 Political Ramifications	70
6.3.5 Ethical Concerns	71

6.3.6 Health and Safety Issues	71
6.3.7 Manufacturability	72
6.3.8 Sustainability	72
7. Discussion	73
8. Conclusion	76
References	78
Appendices	85
Appendix A: USDA Guidelines	85
Appendix B: Extracellular Matrix Extraction Protocol	87
Appendix C: Protocol for Collagen Hydrogel with Single Crowdors	90
Appendix D: MMC Confocal Imaging and Analysis	93
Appendix E: Electrospinning protocol	99

Authorship

Chapter	Written By	
Abstract	Kevin D'Agostino	
1. Introduction	Kevin D'Agostino	
2.1 Fibrotic Phenomena	David Chen	
2.2 Pathophysiology	David Chen	
2.2.1 Extracellular Matrix (ECM)	Kevin D'Agostino	David Chen
2.2.2 Tumor Microenvironment	David Chen	
2.3 Biomaterials used for In Vitro Tissue Models	Vu Nguyen	
2.3.1 Collagen	Vu Nguyen	David Chen
2.3.2 Gelatin	Vu Nguyen	David Chen
2.3.3 Alginate	Vu Nguyen	David Chen
2.3.4 Decellularized Matrix	Vu Nguyen	David Chen
2.4 Current Research	Kevin D'Agostino	Vu Nguyen
2.5 Matrix Modification	Kevin D'Agostino	
2.5.1 Microfluidic Spinning	Kevin D'Agostino	
2.5.2 Electrospinning	Vu Nguyen	Kevin D'Agostino
2.5.3 Macromolecular Crowding (MMC)	David Chen	Kevin D'Agostino
2.5.4 Bioprinting	Vu Nguyen	Kevin D'Agostino
3.2 Design Requirements	Vu Nguyen	David Chen
3.2.1 Objectives	Vu Nguyen	
3.2.2 Constraints	Kevin D'Agostino	
3.2.3 Functions	David Chen	
3.2.4 Means	David Chen	
3.3 Standards	Vu Nguyen	

4.1.1 Methods	Vu Nguyen	David Chen
4.1.2 Materials	Vu Nguyen	David Chen
4.2 Alternative Designs	David Chen	Vu Nguyen
4.2.1 Single Agent Macromolecular Crowding	David Chen	
4.2.2 Mixed Agent Macromolecular Crowding	David Chen	
4.2.3 Electrospinning for 2.5D Scaffold Models and 3D Layering	Vu Nguyen	David Chen
4.2.4 Electrospun Layering within Hydrogel	Vu Nguyen	David Chen
4.3 Final Design Selection	David Chen	
5.1 Turbidity Assay with Macromolecular Crowders	Vu Nguyen	
5.2 MMC Confocal Imaging and Analysis	Yibin Chen	
5.3 Electrospinning	Vu Nguyen	
6.1.1 Ease of Use	Yibin Chen	
6.1.2 Heterogeneous Organization	Yibin Chen	
6.1.3 In Vivo Characteristics	Yibin Chen	
6.1.4 Reproducible	Yibin Chen	
6.1.5 Cost Effective	Yibin Chen	
6.2.1 Decellularization of Pancreas	Vu Nguyen	
6.2.2 Preparation of Collagen Hydrogel with Single Crowding Agents	Vu Nguyen	
6.2.3 Analysis of Hydrogels with Single Crowder	Vu Nguyen	
6.2.4 MMC Confocal Analysis and Imaging	Yibin Chen	
6.2.5 Preparation of Alginate/PEO with Electrospinning	Vu Nguyen	
6.3.1 Economics	Kevin D'Agostino	
6.3.2 Environmental Impact	David Chen	
6.3.3 Societal Impact	David Chen	
6.3.4 Political Ramifications	Kevin D'Agostino	
6.3.5 Ethical Concerns	Kevin D'Agostino	
6.3.6 Health and Safety Issues	Kevin D'Agostino	

6.3.7 Manufacturability	Kevin D'Agostino	
6.3.8 Sustainability	Kevin D'Agostino	
7. Discussion	Yibin Chen	Kevin D'Agostino
8. Conclusion	Kevin D'Agostino	

List of Figures

Figure 1: Histological sectioning of healthy pancreatic tissue vs fibrotic pancreatic tissue.....	13
Figure 2: Schematic of macromolecular crowding process of hydrogels.....	45
Figure 3: Concept of layering electrospun products to create 3D scaffold.....	47
Figure 4: Concept of layering electrospun product within a hydrogel to create a 3D scaffold....	48
Figure 5: Turbidity assay results for type I collagen with crowding agents	51
Figure 6: MMC Confocal images of type I collagen	53
Figure 7: Directionality Histograms	55
Figure 8: Pore size Histograms	56
Figure 9: Confocal images of control and Ficoll 70	57
Figure 10: Shear storage and loss modulus at different alginate: PEO ratios	59
Figure 11: Electrospun product of alginate and PEO	60
Figure 12: Schematic representation of decellularized ECM hydrogel process.....	65
Figure 13: Example of a turbidity graph with label parameters.....	67
Figure 14: Schematic of well plates set up with 1 mg/mL of collagen.....	92
Figure 15: Menu location of “8-bit” tab.....	94
Figure 16: Menu location for “directionality” tab.....	94
Figure 17: Menu path for selecting “8-bit”.....	95
Figure 18: Menu path for locating “Set scale” and “Remove scale”.....	95

Figure 19: Menu path for “Bandpass Filter”.....	96
Figure 20: Menu path for selecting “Auto Threshold”.....	96
Figure 21: Selecting and duplicating an image.....	97
Figure 22: Menu path for “Threshold”.....	97
Figure 23: Setting for Porosity in Threshold.....	98
Figure 24: Menu path for selecting “Analyze Particles” and “Display Result”.....	98

List of Tables

Table 1: Comparison of natural vs synthetic biomaterials.....	21
Table 2: Pairwise Comparison for the Evaluation of Objectives.....	34
Table 3: Pugh Analysis of Methods.....	40
Table 4: Pugh Analysis of Extracellular Matrix Materials.....	42
Table 5: Polymerization Kinetics of Collagen with Crowding agents	52
Table 6: Directionality of different groups of crowding agents in different concentration.....	54
Table 7: Pore size analysis of different groups of crowding agents.....	56
Table 8: Comparison of MMC control group and Ficoll 70.....	58
Table 9: Functions and Means of Design Requirements.....	64
Table 10: Parameters on how electrospinning was run using Alginate/PEO solutions.....	69
Table 11: Fixed and changing parameter of electrospinning.....	99

Acknowledgements

The team would like to thank the following WPI faculty, staff, and graduate students who helped with the development and research of this design project:

- **Project Advisor:** Catherine F. Whittington, Ph.D
- **Biomedical Engineering Department Faculty:** Jeannine Coburn, Ph.D; Marsha W Rolle, Ph.D; Lisa Wall
- **Other Faculty and Staff:** Nancy Burnham, Ph.D; Victoria M. Huntress
- **Graduate Student:** Athenia Jones

The team would especially like to acknowledge Dr. Catherine Whittington for her guidance and support in the terms of design planning and experimentation, as well as with presentations and deliverables. The team would also like to give special thanks to Lisa Wall for her assistance with ordering laboratory materials and acquiring necessary laboratory equipment. Furthermore, we would like to recognize the Rolle Lab for providing the team with a tissue homogenizer and electrospinning device. Similarly, we would like to thank the Coburn Lab for access to their laboratory space and lyophilizer. We would also like to thank Nancy Burham for AFM training and Victoria M. Huntress for confocal training, also Athenia Jones for confocal microscopy and data analysis. Finally, we would like to thank Adam's Farm for generously working with the team and providing special services for procuring porcine pancreata.

Abstract

Fibrosis is pathological wound healing where sustained epithelial cell damage causes an overgrowth of connective tissue. This process leads to excessive tissue remodeling and scarring that can lead to total organ failure in the worst cases. Approximately 360,000 fibrosis-related cases arise in the U.S. alone, and about 54,000 of those cases occur in pancreatic cancer. Current in vitro models of fibrosis often lack the spatial heterogeneity observed in the tissue microstructure (e.g., fibril density, fibril alignment) that influences certain cell behaviors. The team was tasked with creating a 3D in vitro extracellular matrix with heterogeneous fibril density, alignment, and interstitial spacing that could be used for a pancreatic tumor model. The team pursued macromolecular crowding (MMC) and electrospinning techniques to replicate the fibrotic pancreatic tumor environment. Alginate, type I collagen, and pancreas-derived ECM (porcine) were chosen as candidate extracellular matrix (ECM) materials to be used with those techniques. Type I collagen was combined with single MMC agents at different concentrations to determine effects on polymerization (turbidity test) and microstructure (image analysis). Polyethylene oxide and alginate were electrospun to form heterogeneous ECMs for feasibility and proof of concept.

1. Introduction

Fibrosis is the excessive growth, hardening, and scarring of various tissues and organs. This phenomenon is attributed to an abundance of secreted extracellular matrix (ECM) components, including collagen (Wynn, 2008), and can be categorized as reactive, benign, or pathological. In pathological conditions, fibrosis contributes to disease progression and low drug penetration due to high density tissue caused by excess ECM deposition (Choi et al, 2013). Examples of fibrotic diseases and diseases with fibrotic elements include: cancer, primary biliary cholangitis, scleroderma, and idiopathic pulmonary fibrosis in the liver. Fibrotic-related diseases account for 45% of total fatalities in the U.S. yearly and 20% of cancer cases in the country are attributed to fibrosis (Pancreatic Cancer - Statistics, 2019).

Since fibrosis is an integral function of the body's natural defense and repair mechanism in vivo, fibrotic diseases affect the majority of the body's organs (Rosenbloom et al, 2017). The functional cells of the afflicted organ will be replaced with collagen-rich scar tissue which can cause loss of organ function (Shimzu, 2008) (Figure 1), but ultimately every organ is impacted differently. Scarring occurs from sustained injury to the epithelium causing the overproduction of cytokines and growth factors which promote the recruitment and activation of mesenchymal cell precursors to form myofibroblasts. Myofibroblasts are connective cells with a phenotype that is between smooth muscle and fibroblasts, and they are responsible for producing ECM proteins. Since the myofibroblasts form at an unchecked rate, the ECM proteins within connective tissue become heterogeneously distributed with randomly organized extracellular collagen fibers (Hinz, 2016). Myofibroblasts can also be contractile, and this intracellular contraction aligns the newly

produced collagen fibers through integrin-mediated pulling of the collagen bundles. Moreover, this alignment is tantamount to dictating cellular responses such as migration, expression, and secretions (Gnutt et al, 2015).

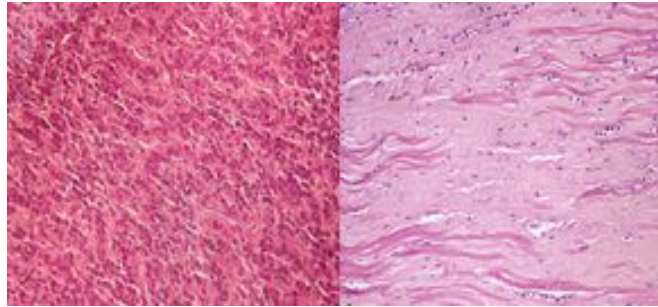


Figure 1: Histological sectioning of healthy pancreatic tissue (left) versus fibrotic pancreatic tissue (right) stained with hematoxylin and eosin (Genten, 2016).

Fibrosis also contributes to cancer progression. Arising evidence suggests a major source of myofibroblast-mediated fibrosis is through transdifferentiation from non-malignant epithelial or epithelial-derived carcinoma cells through epithelial-mesenchymal transition (EMT) (Radisky et al, 2007). Of the organs to be impacted by fibrotic cancer, the pancreas is commonly affected. Roughly 360,000 new fibrosis-related cancer cases arise each year, with 54,000 being pancreatic cancer (Pancreatic Cancer - Statistics, 2019). These patients have low five year survival rates and few treatment options once surgery has been ruled out. Therefore, there is a need to produce better models of the fibrotic elements of pancreatic cancer.

In an attempt to better understand fibrotic phenomena, oncologists have conducted in vitro and in vivo studies. In both of these methodologies, the pathology of fibrotic diseases can be modeled within a system within and outside of a living organism (Feigin et al, 2016). In vitro disease models are fabricated and studied outside of a living system while in vivo models allow for diseases to be observed and manipulated within a living system. Given the prominent role of

the ECM in pancreatic cancer progression, recent in vitro pancreatic cancer models often include ECM components as part of the model system.

Scientists have been striving to more accurately recreate in vivo conditions using in vitro models to better simulate the migration and interactions of pancreatic tumorigenesis. Current in vitro models are often homogeneous in their ECM composition, stiffness, and organization, so they struggle to represent the heterogeneity observed in pancreatic tumor tissue in vivo. ECM organization is a prominent feature of pancreatic tumor tissue and includes variable fibril density and fibril alignment (Gershenson et al, 2011, Whatcott et al, 2012). The highly dense and disorganized ECM contributes to tumor progression and low drug penetration but may also have some protective elements. However, this tissue property is one that is most often missing from in vitro pancreatic tumor models. To accurately recreate a fibrotic environment in vitro for pancreatic tumors, an effective model must incorporate heterogeneity in ECM organization and stiffness observed in vivo.

A variety of approaches have been used to tailor the architectural characteristics of biomaterials in vitro to approximate the properties of native ECM observed in vivo (Magno et al, 2017). A technique like macromolecular crowding (MMC) uses macromolecule size and/or concentration to exclude scaffold material volume to control fibril density, but stiffness often changes at the same time (F et al, 2017). Alternatively, electrospinning and microfluidic spinning are more appropriate for fabricating nano and microscale fibers, while bioprinting allows for more precise control over fiber patterns (Vigier et al, 2016). However, those three approaches require additional equipment.

Given the current needs for improved in vitro models of fibrotic diseases, including pancreatic cancer, and current gaps in modeling capabilities, the team was tasked to design an in vitro model of fibrosis with the ability to induce and maintain heterogeneous features such as fibril organization and scaffold stiffness. If successful, this model will allow for researchers to better comprehend the interactions present in pathological fibrotic environments. In addition, there should be a way to analyze heterogeneity. To achieve these goals, the team conducted investigation and analysis of various materials, laboratory techniques, and verification methods to ensure project objectives were met.

2. Literature Review

2.1 Fibrotic Phenomena

The prevalence of pathological fibrosis in pancreatic cancer has led to a more focused research on the effects on tumorigenesis. The focus placed emphasis on the relationship between the heterogeneous composition and organization of the fibrotic microenvironment and tumor metastasis-related signaling. Pancreatic tumors exhibit the most fibrous and stiff tumor microenvironments, and researchers have already noted its significance in promoting cancer progression (Rice et al, 2019, Bösch et al, 2018). This insistent deposition of ECM is a prominent pathological characteristic of pancreatic cancer described as desmoplasia. Desmoplasia is identified by the dramatic increase in proliferation of alpha-smooth muscle actin-positive fibroblasts accompanied by the telltale excessive deposition of many ECM components such as type I collagen and fibronectin (Whatcott et al, 2012). A 2017 study utilized genetically modified mice to model the pancreatic tumor microenvironment to investigate the desmoplastic response observed in pancreatic cancer (Rice et al, 2017). They found that the recapitulation of the fibrotic rigidities found in pancreatic tumor tissue promoted elements of epithelial-mesenchymal transition (EMT), a cellular mechanism that precludes metastasis and that has been tied to pathological fibrosis and cancer progression (Lamouille et al, 2014). Moreover, they explored the effect of ECM stiffness on EMT and chemoresistance. Since those studies were performed, others have also linked fibrosis with the spread and progression of pancreatic tumors.

2.2 Pathophysiology of Fibrosis

2.2.1 Extracellular Matrix (ECM)

The emphasis on ECM composition, structure, and stiffness in fibrosis is due to its dysregulation throughout the fibrotic process. Collagen, the main structural protein in the body's connective tissues, is classified into fibrillar (types I–III, V and XI) and non-fibrillar forms (types VI, VIII, XVII). Collagen fibrils provide tensile strength to the ECM, limiting the distensibility of tissues (Bonnans et al, 2014). ECM is divided into two categories: the basement membrane and the interstitial tissue matrix. The basement membrane is a specialized form of ECM separating epithelium from the surrounding stromal tissue. It also controls cell organization means such as polarity and differentiation through interactions with surface receptors (Bonnans et al, 2014). The interstitial matrix surrounds cells in a mesh-like network and is mainly composed of collagen I and fibronectin in many of the body's tissues but other macromolecules also exist in varied amounts depending on the tissue. Both provide structural scaffolding for tissues and have inherent signaling capabilities.

By taking the crucial function of ECM components into account, certain processes surrounding fibrotic progression can be more easily understood. The primary mechanism behind excess deposition of myofibroblasts is the suppression of miR-29, a master negative regulator of ECM genes (Herrera et al, 2018). The loss of the negative feedback loop results in autonomous function, and suppression results in a positive probiotic feedback loop that promotes further fibrosis.

Progression of the pathological fibrosis wound healing also produces changes in mechanical properties (e.g., viscoelasticity) of the ECM. Due to the dense, fibrous nature of pancreatic fibrotic tissue, the ECM becomes stiffer than the normal value of 1kPa at around 2kPa on average (Watt et al, 2013). These changes in ECM stiffness play an important biological role by influencing mechanotransduction, a process by which extracellular mechanical stimuli are converted to intracellular biochemical signalings. Mechanotransduction pathways impact prominent cellular functions such as proliferation, differentiation, and cell migration. A 2017 study showed a progression from a healthy pancreas exhibiting a Young's Modulus of 1kPa to a modulus of 4kPa with prevalence of pancreatic ductal adenocarcinoma (PDAC) (Rice et al, 2017). Histograms compiled for the stiffness showed more consistent high moduli in cases of PDAC, providing implications of mechanotransduction alterations due to fibrosis (Rice et al, 2017).

Dimensionality of an in vitro model can also impact cellular response to viscoelastic properties. Studies have shown ECM stiffness in both 2D and 3D systems impacts translocation of yes-associated protein (YAP). YAP is a transcriptional coactivator that interacts with other transcription factors to control cell growth (Nishimoto et al, 2019). Manipulating the elasticity of the ECM through means such as ligand binding has shown to inactivate YAP because of signaling disruptions to adhesion sites. This causes a reduction to the rate at which fibrotic tissue is produced (Herrera et al, 2018).

Even though certain features of fibrosis uniquely affect the pathophysiology in vivo, there is still difficulty in exercising control over those features in vivo and in vitro. In addition, the means as to which researchers are manipulating matrix density and elasticity is still

ill-defined. Thus, further investigation of laboratory techniques that allow controlled manipulation of structural properties is needed.

2.2.2 Tumor Microenvironment (TME)

The tumor microenvironment (TME) is a significant point of interest among researchers in recent years, because more evidence has been shown to directly influence tumor metastasis and progression. The tumor microenvironment is composed of stromal cells (endothelial cells, stromal macrophages, fibroblasts, etc.) and acellular compartments consisting of ECM macromolecules and cytokines. One 2013 study published findings that the abnormal TME fuels tumor progression (Jain et al. 2013). Specifically, they focused on how the combination of abnormal stromal cell density, angiogenesis, and ECM concentrations of TME resulted in a hypoxic (low oxygen) environment that has already been established to induce further fibrosis and angiogenesis in pancreatic cancer (Masamune et al. 2008). This positive feedback loop of fibrosis inducing hypoxia, and hypoxia inducing more fibrosis in the pancreas, greatly contributes to the aggressive nature of fibrotic cancers.

The heterogeneous composition of TME also poses other issues for researchers. In fibrotic cancers, fibrotic tissue that surrounds the primary tumor often results in decreased drug penetration due to its highly dense, stiff make-up (Choi et al, 2013). Another study also found the heterogeneous TME contributed to a fibrosis-mediated chemoresistance (Zeltz et al, 2019). The compact and stiff fibril networks diminish nuclear accumulation of the chemotherapeutic agent resulting in the lowered effectiveness of certain chemotherapies on fibrotic cancers (Akkari et al, 2016, Wang et al, 2016).

The connection between the TME and aggressive tumor development has been established in many studies. Researchers are focusing efforts in identifying potential therapeutic targets to halt the desmoplastic cascade associated with exocrine pancreatic tumors but are thwarted by the complexities of the TME. The team saw a need for an in vitro model that incorporates the heterogeneous characteristics of the pancreatic TME for better representation of the in vivo condition.

2.3 Biomaterials used for In Vitro Tissue Models

The choice for biomaterials used to create in vitro tissue models often depend on the organ and tissue being modeled. The most common type of materials used to model pancreatic tissue, including the TME, are made with natural or synthetic polymers. The team evaluated synthetic and natural polymers in terms of their advantages and disadvantages within the context of pancreatic TME modeling (Table 1).

Table 1: Comparison of natural vs synthetic biomaterials as tissue model base materials

	Synthetic Biomaterials	Natural Biomaterials
Advantages	Tunable biodegradation, biocompatible, tunable mechanical strength (Dhandayuthapani et al, 2011)	Biodegradable, biocompatible, low toxicity, bioactive motifs, mimic ECM (Dhandayuthapani et al, 2011; Garg 2011)
Disadvantages	Inflammatory response, generally hydrophobic (Gazia et al, 2019; Salg et al, 2019)	Immunogenicity, little to no control over degradation, poor mechanical properties, variation between batches (Garg, 2011; Kumar et al, 2018)
Examples of in vitro scaffold modeling	Additive manufacturing using PLA (Wurm et al, 2017) PEG mediated fusion of the nerve cells (Messineo et al, 2019)	Collagen invasion model for drug screening (Puls et al, 2018) Cell immobilization using Alginate (Andersen et al, 2015)
Common materials	Polylactic acid (PLA), Polyglycolic (PGA), Polylactic-co-glycolic acid (PLGA) poly(ethylene glycol) (PEG) (Kumar et al, 2018; Salg et al, 2019)	Collagen, Gelatin, Fibrin, Alginate, Silk (Kumar et al, 2018)

2.3.1 Collagen

To recreate the ECM of mammalian tissues in vitro, it is important to consider using one of the most prominent polymers found in the ECM. Type I collagen is a natural polymer that has been widely used for 3D cell culture and modeling tissues in vitro. The hierarchical structure of collagen—triple helical collagen molecules that assemble into collagen fibrils and fibers—allows its physical properties to be influenced by temperature and pH to polymerize into a hydrogel in vitro. Type I collagen is acid-soluble and consists of molecules in the shape of thin rods when under storage conditions (<10°C). However, as the environmental conditions near that of

physiological conditions with neutral pH (~7.4) and body temperature (37°C), collagen begins to polymerize to self-assemble into fibrils to form a hydrogel. Type I collagen has many desirable properties such as being biocompatible, biodegradable, and non-toxic. It is widely used for cell adhesion, and though the mechanical strength of collagen is poor compared to natural tissue and some synthetic polymers, collagen mechanics can be adjusted by varying the concentration of collagen or through collagen glycation or crosslinking (Mason et al, 2013).

The Puls 2017 study used collagen to represent the interstitial matrix and Matrigel to represent the basement membrane for an in vitro pancreatic tumor model (Puls et al, 2017). The phenotype of the pancreatic tumor cells, that varied in their invasive potential, was guided based on the type of material they were in and the respective material properties. Since fibrosis produces varying tissue stiffness, they capture the response of tumor cells in different stiffness environments. The protein composition in fibrosis also differs from normal tissue, so the interaction of cells in different protein composition environments is also a consideration when modeling fibrosis. However, collagen is always found in fibrosis. Since collagen is one of the most abundant polymers found in tissue ECM and is used for in vitro models of many tissues, it is considered to be a golden standard for in vitro models (Sung et al, 2009).

2.3.2 Gelatin

Another possible way to mimic the ECM is to use gelatin, which is the denatured form of type I collagen. Gelatin has a similar chemical composition as collagen but requires additional chemical cross-linkers such as glutaraldehyde or methacrylic anhydrides to maintain its structure at physiological temperature (37°C) and tune mechanical properties to better match the in vivo

tissue environment (Kwak et al, 2018, Jumar et al, 2018). Just like collagen, gelatin is biocompatible, biodegradable, and non-toxic. It contains an Arginyl-Glycyl-Aspartic Acid (RGD) sequence that is used for cell attachment, and enzymatic degradation sites making this polymer ideal for cell culture, cell adhesion, and cell entrapment. A 2010 study utilized gelatin for 3D scaffold for tissue models (Xu et al 2010). They sought to address the still present lack of 3D in vitro models for analysis, and ultimately recognized the potential of gelatin as a scaffold material but concluded the application is limited due to their poorly controlled structure (fiber clusters, pore size etc). Another study performed in 2016 aimed to address the same lack of in vitro 3D ECM models (Loessner et al, 2016). A mixture of denatured and partially hydrolyzed collagens (primarily type I collagen) derived from animal tissues was utilized for the 3D ECM mimic model. The study concluded such a model could be reliably fabricated for reproducibility (characterized via cell proliferation and matrix stiffness).

Gelatin has been used in pancreatic cancer, and introduces heterogeneity into a system. For example Liu 2018 fabricated a dynamic gelatin-hyaluronic acid hydrogel (Liu et al, 2018). Here gelatin was modified to capture the progressive stiffening observed in pancreatic tumor desmoplasia, and how that would influence COLO-357 cells (metastatic pancreatic adenocarcinoma cells). Since fibrosis is progressive, it is important that researchers also consider emulating this dynamic nature of stiffing. Another example is Saxena 2005 who used different molecular weight gelatin to study the size and stability of nanoparticles (Saxena et al, 2005). Though this study does not relate to a pancreatic, it does highlight the ability to manipulate gelatin structure in a way that could be considered to introduce heterogeneity for the proposed system.

2.3.3 Alginate

Alginate is another natural biomaterial that is low cost, and biocompatible. By exposing it to divalent ions like Ca^{2+} , Ba^{2+} , or Sr^{2+} , alginate is able to form a hydrogel that encapsulates cells. However, alginate would need to be functionalized with a RGD sequence or coated with another protein (e.g., gelatin, fibronectin) to promote cell adhesion and proliferation, because mammalian cells lack surface receptors that can bind to alginate (Klontzas et al, 2019). Alginate has also been widely used to investigate many material features such as stiffness, viscoelasticity, and porosity, which can all be used to better understand the nature of fibrosis (Davidson et al, 2020).

A study has been performed with alginate and polycaprolactone to fabricate a multi-layer heterogeneous scaffold using bioMED_{Beta}, a manufacturing system that can be used to produce heterogeneous 3D structures for tissue substitutes (Biscaia et al, 2017). Though this work did not directly apply to the pancreas, it does demonstrate the possibility of using alginate as a natural material to create the heterogeneous architecture found in the ECM. Another study was performed with chitosan and alginate scaffolds for prostate cancer cell lines (Xu et al, 2019). Scaffolds of different stiffness and pore size were used to study this response. Although alginate is often used for drug delivery applications, these studies expand the applications of alginate to use it to study cancer and heterogeneity found in the ECM.

2.3.4 Decellularized Matrix

To obtain a better representation of the ECM of specific tissues, decellularizing tissues or organs would allow for the incorporation of multiple natural ECM macromolecules in a single

material. Dependent on the original tissue, these macromolecules can include type I collagen, other collagen types, laminin, fibronectin, and glycosaminoglycans (GAGs). Not only will these macromolecules provide structural support, they will also influence cell morphology and cellular functions such as adhesion, proliferation, differentiation, and migration. Collagen rich decellularized ECM behaves similarly to type I collagen when forming hydrogels in vitro. Acid solubilization followed by exposure to neutralization buffers and physiological temperature will induce polymerization. With the different macromolecules making up the overall ECM composition, decellularized ECM has potential to be an ideal biomaterial for in vitro modeling (Sackett et al, 2018). For example, a study has decellularized human pancreas to fabricate hydrogel, and reported over 120 proteins that are present (Sackett et al, 2018). Many models only account for a few proteins found in the ECM, but with decellization, many more proteins can be accounted for a better representation. In a review, decellularized ECM has many advantages over current in vitro testing platforms as it captures the biomechanical and biomolecular complexity of the tumor ECM (Ferreira et al, 2020). It also discusses the possibility of decellularization of patient-derived tissue-specific samples to capture the composition variation between patients. Furthermore, sourcing of decellularized ECM can be from various tissues, including fibrotic tissue, and thus can target the matrix composition best matched based on the molecular composition of the tissue being studied (Porzionato et al, 2018)

2.4 Current Research

With fibrotic diseases greatly adding to modern-day mortality, significant preclinical modeling improvements must be made to better treat fibrotic diseases (Rosenbloom et al, 2017).

Both a combination of 2D and 3D techniques are used to replicate fibrosis conditions seen in affected sites. Commonly, 2D studies rely on activation of fibroblasts in monolayer on a tissue culture plastic (TCP). Primary fibroblasts, upon culturing on TCP or with transforming growth factor- β (TGF- β) treatment, transdifferentiate into a highly proliferative, contractile, and ECM producing myofibroblasts (Sacchi et al, 2020). With the ability to induce myofibroblast formation, ECM alignment and density of related tissue may be able to be analyzed if the cells secrete their own ECM. A limitation in 2D applications is the ability to fully replicate the in vivo fibrotic conditions. The in vivo environment is 3D, and in vitro stiffness ranges on the order of GPa, due to the TCP, compared to in vivo stiffness ranges on the order of kPa. The differences in stiffness value suggest the in vitro mechanical environment of 2D models does not replicate anatomical tissue properties (Sacchi et al, 2020). In addition, 2D models fail to truly mimic the 3D fibrotic microenvironment and related processes.

Current 3D model systems have seen the use of bioprinting emerge as a popular approach. In order to provide a highly tissue-specific microenvironment, specific-organ-derived decellularized ECM (dECM)-based bio-inks have been developed (Sacchi et al, 2020). By combining renal dECM with different hydrogel materials, such as gelatin, hyaluronic acid, and glycerol, a printable ink has been developed incorporating organ-specific cells including proximal and distal tubular epithelial cells (PTECs/DTECs) and podocytes. The 3D-bioprinted construct provides structural integrity as well as a tissue-specific microenvironment. Hydrogel materials along or with cells have also been used often for 3D bioprinted models.

Type I collagen has also been used to mimic the TME in the pancreas 3D. For example, Puls 2018 uses collagen to represent the interstitial matrix (Puls et al, 2018) in a tissue

compartment surrounding a spheroid-like tumor compartment. They varied the interstitial matrix stiffness and quantified the number and distance that PANC-1 cells, a moderately invasive pancreatic tumor cell line, invaded from the tumor compartment into the surrounding matrix. This model supported 3D radial invasion, which was more in vivo-like compared to more traditional invasion models like exclusion zone assays or Boyden chambers (Kramer et al, 2013). Though the ECM in the Puls study was homogenous in microstructural organization and stiffness, the model mimicked some elements of fibrosis. First, for some experimental groups the stiffness of the ECM in the tumor compartment was lower than the stiffness of the surrounding interstitial matrix, which is similar to increased stiffening in fibrotic tissue. They could capture how cells interact at the interface, with localized stiffness differences, to give more insight on how to better model fibrosis. The interface between the two matrices had different stiffness. The model also had low and high stiffness values for the surrounding interstitial matrix, which mimicked increased tissue stiffness due to fibrosis. 3D models allow for closer representation of the environment it is modeling. However, these models still struggle to incorporate and control heterogeneity in fibril elements such as density and alignment, which contribute to elements like cell phenotype, proliferation, and invasion.

2.5 Matrix Modification Approaches

With numerous potential scaffold materials to model fibrotic processes, there are also multiple techniques used to fabricate in vitro tumor models. Of the current models used for in vitro applications, 70-80% are cell cultured on 2D platforms such as petri dishes and coverslips (Hutmacher, 2010). Three dimensional models are preferred over monolayers to better resemble

in vivo tumors because of the complexities of the TME, including fibrosis. In addition, the pharmaceutical industry needs more pathophysiologically relevant tumor models that are more predictive of the therapeutic response. Tying back into the importance of ECM mechanisms in relation to fibrosis, controlling matrix organization is crucial in understanding how this biophysical property affects the TME.

2.5.1 Microfluidic Spinning

When representing an organ's makeup during fibrosis, it is imperative to generate a fibril 3D fibril network. Microfluidic spinning is one application where fluid flow is directed into microchannels with cells in 3D to then encapsulate them into fiber-like structures after the material solidifies. Microfluidic spun microfibers are long, thin, and flexible, and these features facilitate higher-order assemblies for fabricating cellular structures. This technique has been used to create hydrogel microfibers assembled into a scaffold for 3D vasculature systems (Sun et al, 2018). The use of microfluidic spinning has also been shown to facilitate high porosity and larger pore sizes through manipulation of scaffold size. A 2018 study achieved the porosity and pore size manipulation via different flow types (parallel laminar and coaxial laminar). The focus of this study was on using alginate as a hydrogel material to create a vascular network in vitro (Sun et al, 2018). The different flow types allowed researchers to monitor how fluid would behave in vivo, which can potentially be translated to a cancer study in understanding nutrient flow to the tumor.

2.5.2 Electrospinning

Electrospinning involves the gradual pumping of polymers onto a target surface at a desired voltage to generate fibrous materials/structure. It has a proven ability to randomly generate fibrous scaffolds assembled into nonwoven networks that are deposited in a random fiber orientation (Jun et al, 2018). This technique is desirable for both the ability to closely replicate the pancreatic microenvironment while capturing random fibril orientation. A study was performed that used electrospinning to create a hydrogel scaffold with embedded 3T3 fibroblast cells (Xu et al, 2020). Researchers were able to control the internal morphologies to create different structural architecture, which introduced heterogeneity to their system for the cells to interact. There have also been studies that use electrospinning for its controlled alignment of fiber structures (Thomas et al, 2006). Though the time was trying to look at the heterogeneity of the fiber organization, homogeneous fiber organization is necessary for comparison. Overall, electrospinning has been used to create scaffolds that mimic the natural structure found in the ECM, but less work has involved cell encapsulation or the pancreas specifically (Cheng et al, 2017).

2.5.3 Macromolecular Crowding (MMC)

MMC achieves the desired matrix modifications by manipulating protein and macromolecular interaction within a model system to exclude material volume and show the individual impacts of certain molecules on matrix properties. Further impacts can include molecular assembly and ECM protein deposition (Zeiger et al, 2012). A 2011 establishing paper aimed to highlight MMC as a potential tool for matrix engineering (Chen et al, 2011). They

utilized a large variety of crowding agents, which were combined with ECM materials, to study their effects. They concluded that negatively charged crowders with large hydrodynamic radii could effectively induce higher type I collagen aggregates in 48 hours compared to a 6-8 week static system. Furthermore, they noted neutral agents (Ficoll 70 and Ficoll 400) would not prompt a similar increase over the same short time period. However, with the introduction of mixed crowding agents, the combinations of Ficoll 70 and Ficoll 400 “substantially enhanced ECM deposition” over a window of 5 days. Ultimately they concluded that MMC provides an underlooked opportunity for matrix modification, specifically, the utilization of crowding agent mixtures that holds a potential that “has not been fully fathomed”.

In 2017, a study concluded that MMC can be employed for tailoring important structural and biophysical characteristics of kidney-derived fibrillar matrices (Magno et al, 2017). With the introduction of MMC agents into the matrix reconstitution media, researchers demonstrated the ability to adjust fibrillic kinetics and architecture, fiber diameter, alignment and matrix elasticity. They compared their engineered fibrotic matrices against specific kidney tissue engineering requirements (predominantly cell response) as proof of concept. A 2019 study established another approach to manipulating type I collagen matrices for breast cancer applications using low molecular weight poly-ethylene glycol (PEG) as a crowding agent during gelation (Ranamukhaarachchi et al, 2019). They found they were able to induce tighter fibril networks that were less susceptible to degradation, factors they concluded were strong predictors of cell response. The researchers chose to use a low molecular weight crowding agent at varied concentration to alter fiber microstructure but not significantly change ECM stiffness, which is usually confounded with higher molecular weight agents.

2.5.4 Bioprinting

Bioprinting combines ECM, cells, and sometimes growth factors to create tissue-like structures that protry fibril structures. This process can produce a microenvironment conducive to the growth of 3D structured tissue with bioink from dECMs (F et al, 2017), as well as other natural or synthetic polymers. This process allowed added control over fibril density to study fibrosis. A study involved three different fabrication modules to print heterogeneous structures using natural and synthetic polymers. They demonstrate the possibility of being able to obtain these well-defined architectures found in the ECM, but the technique is still under development for constructing a higher number of layers for the scaffold (Biscaia et al, 2017). In another study, the liver architecture was mimicked by 3D bioprinting decellularized liver hydrogel for a more relevant physiologically and mechanical environment (Ma et al, 2018). This study shows the possibilities of bioprinting to fabricate tissue-specific organs, and capturing the architecture found in these environments.

3. Project Strategy

3.1 Client Statement

The initial client statement was provided by the project advisor as follows: *“To design an in vitro model system with a controlled spatial organization that yields characteristic heterogeneities found in fibrotic disease conditions and can be integrated into higher throughput screening protocols.”* The focus of heterogeneities was heavily enforced considering the current gap in the field in regards to in vitro models of fibrosis, particularly fibrosis-related cancers. After conducting a literature review and developing design objectives, constraints, and functions, the initial client statement was expanded and revised to better fit client and project needs.

3.2 Design Requirements

Upon reviewing the initial client statement, the team developed a list of primary objectives that addressed the crucial aspects of what the design should be or should have:

3.2.1 Objectives

1. Ease of use: The purpose of this objective is to ensure the model should be easy to handle, which includes the ability to be sterilized in a conventional research laboratory and short overall preparation time. In addition, the design should be prepared to easily analyze for fibrotic features.

2. *Heterogeneously organized*: The purpose of this objective is the ability to tailor microenvironments to have features resembling those observed in fibrotic tissue for improved modeling (e.g., pancreatic tumorigenesis). The in vitro model should have varied degrees of ECM density (e.g., crowding, fibrillar spacing) and fiber alignment synonymous with tumor microenvironments in vivo.

3. *In vivo characteristics*: The purpose of this objective is to use a combination of materials and approaches that produce macromolecule composition, mechanical properties, and/or organization similar to what is found in vivo.

4. *Reproducible*: The purpose of this objective is to ensure the approaches and techniques used to create the engineered ECM can be utilized by others outside of the project team to generate similar results.

5. *Cost effective*: The purpose of this objective is to balance project costs with efficacy. The total cost for materials and equipment for the fabrication and implementation of the design should not exceed the \$1000 budget outlined for the project.

After additional discussion with the project advisor and reviewing literature, the objectives were prioritized and organized in terms of value using a pairwise comparison chart (Table 2).

Table 2: Pairwise Comparison for the Evaluation of Objectives

Objective	Ease of use	Heterogeneous organization	In vivo characteristics	Reproducible	Cost efficient	Total
Ease of use	x	0	0	0	0	0
Heterogeneous organization	1	x	1	1	1	4
In vivo characteristics	1	0	x	1	1	3
Reproducible	1	0	0	x	0	1
Cost efficient	1	0	0	1	x	2

The objectives were evaluated based on their overall priority and importance to obtaining project goals and satisfying the needs outlined in the client statement. To determine the significance of each of the objectives relative to one another, each objective is evaluated on a scale of 0 to 1 to compare objectives in the left column compared to objectives in the top row for lesser (0) or greater (1) priority. Thus, each objective was compared to each of the others in a pairwise analysis chart .

In this chart, using the pairwise comparison, the objectives “heterogeneous organization” and “in vivo characteristics” (scores highlighted in yellow) emerged as the two most important criteria for our design to create an in vitro model. As our client stated, they are looking to design an in vitro model with characteristic heterogeneities found in fibrotic tissue. It is important to find ways to create this heterogeneous organization, and make sure it has the in vivo characteristics to the disease that we are looking at in an in vitro model. Therefore, these became our areas of focus in the process.

3.2.2 Constraints

To design our system based on client needs and satisfy the design objectives, the team identified a list of constraints. These constraints are utilized as a cut-off for the success of the design. If a design failed to meet any of the constraints, that design iteration would be considered a failure:

1. Engineered matrix must exhibit statistically significant heterogeneity: Engineered matrix must exhibit heterogeneous fibril directionality, density, and porosity at a confidence level of 80% or greater (Lih Loh et al, 2017) when compared to homogeneous matrices.

2. Engineered matrix fibers are stiff enough to maintain structure: The in vitro model requires a Young's Modulus in the range of 1kPa to 4 kPa to ensure the engineered matrix will be structurally sound (Rice et al, 2017). Furthermore, this range encompasses the mean stiffness of normal and cancerous pancreatic cells environments (Masamune et al, 2009).

3. The model must be biocompatible: The model cannot induce cell death nor inhibit cell expression while still inducing heterogeneities in the scaffold. Biocompatibility relates to the chosen materials and their physical properties. Thus, the model must exhibit cell viability of 80% at minimum (Ghorbani et al, 2015). Higher cell viability is desired to appropriately study cellular behavior, including specific cell mechanisms.

4. Model must be inexpensive: After fabrication, testing, and validation, this model should not put the project over the \$1000 budget. This amount also includes costs related to material and reagent purposes, as well as equipment costs (e.g., purchase, usage fees).

3.2.3 Functions

Upon the evaluation of the objectives and constraints, the team identified functions to define the various parameters needed to fulfill the design requirements. The functions are as follows:

- 1. Simulate in vivo pancreatic ECM stiffness, interstitial spacing, and fiber organization:* To accurately model the pancreatic TME in vitro, the model must simulate the in vivo ECM conditions.
- 2. Model for both 2D and 3D fibrotic pathology analysis:* Model must be able to be fabricated in 2D or 3D based on the need of researchers.
- 3. Retain physiological conditions for accurate modeling:* Not hinder or influence cell response to scaffold.

The first function the design should fulfill is the simulation of in vivo pancreatic ECM stiffness, interstitial spacing, and fiber organization. This applies to various ECM stiffnesses, interstitial spacings, and fiber organizations depending on the organ or tissue being simulated. The next function to be considered is the ability to be utilized for both 2D and 3D fibrotic pathology modeling. This is to ensure the model can be adapted and utilized for differing data analysis objectives. The final function our design should have is the retention of physiological conditions for accurate modeling. The model should not unintentionally influence cell response nor result in low cell viability.

3.3 Standards

To ensure the safety of our final device, standards put in place by the International Standardization Organization (ISO) and the American Society of Testing and Materials (ASTM) will have to be met for the project to be successful. The decellularized ECM and the crowding agents will have to be sterilized and testing of sterility will be needed based on ISO 11737-2:2009 “Sterilization of medical devices”. This ensures that accepted procedures for sterilization for the extracted material and the crowding agents can be performed before adding cells into our models.

The in vitro model will have to be tested for cytotoxicity based on the ISO standard 10993-5:2009 “Tests for in vitro cytotoxicity”. Because the use of decellularized ECM from a pig, crowding agents, and cells, the model system cannot be cytotoxic due to potential influence on the data collection. This test will ensure the byproduct release through diffusion or degradation from the extracted material or crowding agents will not be toxic to cells. The in vitro model will have to be tested for biocompatible based on the ASTM standard F2739-16 “Standard Guide for Quantifying Cell Viability within Biomaterial Scaffolds”. As cells are incorporated into this model, testing will quantify the cell viability. The test will indicate the in vitro model is not harmful to when cells are in contact.

3.4 Revised Client Statement

From further refining and improved understanding of project goals and constraints, the initial client statement was revised to better encompass client needs. The reconstituted client

statement reads as follows: *“To design an inexpensive and reproducible 3D in vitro pancreatic tumor model with tailored heterogeneities for a variety of research settings. The model should control ECM concentration, fiber organization, and interstitial spacing to yield better physiological accuracy.”*

4. Design Process

4.1 Needs Analysis

4.1.1 ECM Manipulation Methods

After the team conducted a literature review of relevant methods that could be used in our design, a Pugh Analysis (decision matrix) was created (Table 3). This decision matrix includes the objectives outlined in Section 3.2.1 as criteria for the decision. The weight of each criteria was ranged between 1 through 5. Heterogeneous organization had the weight of 5 as it was the most important criteria to ease of use having the weight of 1 as it was the least important criteria. These techniques were ranked against a type I collagen hydrogel that has been neutralized, pipetted into a multiwell plate, and fully polymerized at 37°C. This collagen preparation is commonly used to mimic the ECM of various tissues, including pancreatic tumors, and has a homogeneous distribution of fibers and stiffness. Each approach was given a score from -1 to 1 for each objective with a 1 showing greater than baseline, a 0 showing the same as the baseline, and a -1 showing worse than the baseline.

The methods designs as discussed in Section 2.5 that were scored in this decision matrix were: Microfluidic spinning (fluid flow into microchannels with cells and encapsulate them into fiber-like structure), Electrospinning (the usage of electrostatic force to transform liquid polymers into fiber structure), Macromolecular crowding (MMC; Inducing volume exclusion effects via macromolecular beads in solution), and bioprinting (additive manufacturing of

biomaterials to mimic tissue and organs structure). Electrospinning and MMC scored the highest in the Pugh Analysis and deemed most feasible for the project. The factors that contributed most to these outcomes were the cost efficiency. Both microfluidic spinning and bioprinting received a -1 for both devices were not available to us and purchasing or building was not an option. Electrospinning and MMC received a 1 for being inexpensive and/or available for use based on equipment already available to the team.

Table 3: Pugh Analysis of Methods

Objective	Weight	Baseline	Microfluidic Spinning	Electrospinning	Macromolecular crowding	Bioprinting
Ease of use	1	0	-1	-1	0	-1
Heterogenous organization	5	0	1	1	1	1
In vivo characteristics	4	0	1	1	0	1
Reproducible	2	0	0	-1	0	0
Cost efficient	3	0	-1	1	1	-1
Score			5	9	8	5

Ease of use, which had the lowest weight value, related mostly to experience, sterilization, data collection, and/or preparation time. Team member experience was also lacking for microfluidic spinning, electrospinning, and bioprinting. Overall, the process for preparing samples using electrospinning is relatively simple, but involves many different parameters that

would have to be adjusted based on the type of material. Similar concerns were expressed for microfluidic spinning and bioprinting, which was why those methods were scored with -1. The MMC process is well established in hydrogels and has been used for collagen hydrogels. Therefore, the team anticipated that data collection of fiber organization and stiffness would be relatively similar to existing procedures for all candidate materials. .

Heterogeneous organization, which had the highest priority score, related to fiber density alignment, and stiffness. All of the methods are capable of producing heterogeneous fiber organization either by producing fiber-like structures with varied sizes and orientation in sizes (microfluidic spinning, electrospinning, bioprinting) or able to manipulate fiber spacing (MMC), giving them all a 1.

In vivo characteristics, which had the second highest priority score, related to macromolecule composition (e.g., protein, glycosaminoglycan) and biophysical properties (e.g., stiffness, organization) found in vivo. All of the methods considered can be used with different types of materials that are porous upon polymerization or gelation and have tunable mechanical properties depending on preparation procedures. The methods that produce fiber-like structure can mimic fibers that are found in the native tissue microenvironment giving these a 1. Since MMC methods tend to use crowding agents that are not naturally found in the body, MCC received a 0.

Reproducible had the second lowest score, and was primarily concerned with consistent replication of the overall design across multiple users. There was concern that electrospinning would be more difficult to replicate since parameters can change slightly with each use. These

changes would likely produce some variability, so the method was scored at -1. Other methods were deemed on par with the baseline.

4.1.2 ECM Materials

After the team conducted a literature review of candidate materials to use for the design, a Pugh Analysis was performed (Table 4). The weight of each criteria and the baseline were the same as what was used for the methods analysis.

The candidate materials that were evaluated were: Alginate, Gelatin, and Decellularized ECM. The decellularized ECM scored the highest in the analysis and was deemed most feasible for the design. The criteria that contributed most to the scoring were heterogeneous organization and in vivo characteristics.

Table 4: Pugh Analysis of Extracellular Matrix Materials

Objective	Weight	Baseline	Alginate	Gelatin	Decellularized ECM
Ease of use	1	0	1	1	0
Heterogenous organization	5	0	0	0	1
In vivo characteristics	4	0	-1	0	1
Reproducible	2	0	0	0	-1
Cost efficient	3	0	1	1	0
Score			0	4	7

For heterogeneous organization, all candidate materials had a wider stiffness range than commercially available collagen formulations. However, alginate and gelatin would not have visible fiber structure as an engineered matrix unless one of the printing or spinning methods was used. Therefore, alginate and gelatin were scored at 0.

For in vivo characteristics, alginate does not represent characteristics in vivo as it is not a protein found in animals. Alginate would have to be used in combination with another polymer to promote cell attachment, so it was given a -1. Gelatin is the denatured form of collagen, which means protein composition is virtually the same, so gelatin was scored at 0. Decellularized ECM from pancreatic tissue has collagen type I and many other macromolecules found in the tissue, so it was scored at 1.

In regards to ease of use, all materials were considered easy to handle. However, decellularized ECM required additional processing prior to hydrogel preparation, whereas alginate and gelatin were commercially available. Alginate and gelatin also had established protocols for sterilization. Altogether, alginate and gelatin were scored at 1 for ease of use.

For material reproducibility, the team was most concerned with batch-to-batch variability that would be highest in decellularized ECM. Since decellularized ECM would possibly undergo processing multiple times in the laboratory and would be processed from new tissue each time, there were concerns that composition could change somewhat, so that material was scored at -1. The other materials could be sourced commercially like collagen.

Cost efficiency concerned itself with the time, and cost of the material. All these materials are very cheap to produce or to purchase, however decellularized ECM takes much more time to produce giving it a -1.

4.2 Alternative Designs

The team initially began by researching existing studies and their methods of modifying or engineering in vitro models for fibrotic disease. From there we expanded our knowledge of the subject via composing a spreadsheet with important categorical information (materials, methods, results, etc.) from various articles. With a growing list of literature, we began to hypothesize various methods of tackling our revised client statement: Designing a 3D in vitro pancreatic tumor model with controlled ECM scaffold fiber thickness, alignment, and interstitial spacing to yield better physiological accuracy. With our objectives guiding our method fabrication process, our current design alternatives utilize a combination of approaches and materials.

4.2.1 Single Agent Macromolecular Crowding

Macromolecular crowding is a well-established method for inducing exclusion volumes effects (Miklos et al, 2010). Macromolecular crowding agents used for the design could potentially introduce some degree of spatial heterogeneity in an engineered matrix. The team considered using polyethylene glycol (PEG), Ficoll, and albumin as potential crowding agents with varied molecular weight (size kDa). These crowding agents have shown significant potential in altering ECMs in vitro to modulate cellular responses in collagen-based hydrogel formulations, including reconstituted matrices from decellularized ECM (Magno et al, 2017, Ranamukhaarachchi et al, 2019). By introducing various concentrations of different sized single MMC agents into the hydrogel formation process, the team felt that they would be able to

modulate the organization of the engineered matrix to simulate the pancreatic TME. As seen in (Figure 2), crowding agents are mixed with the desired ECM components during gelation to induce matrix modification.

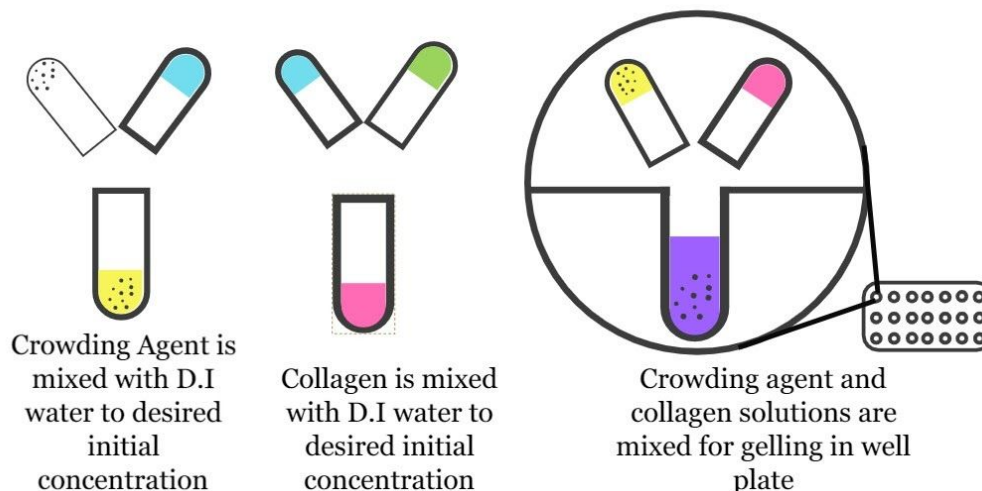


Figure 2: Schematic of macromolecular crowding process of hydrogels

4.2.2 Mixed Agent Macromolecular Crowding

Individual MMC agents have been established to be a robust method for a variety of tissue model applications. Intrigingly, the utilization of mixed crowding agent solutions has only been researched a handful of times. Moreover, it is concluded that the future of applied MMC shows the most promise with combined agents (Chen et al, 2011). The team stayed with the same MMC agents chosen for single agent MMC (PEG, Ficoll, and albumin) to be utilized in combination for more pronounced modulation of ECM matrix cellular response and exclusion effects. Previous studies suggest that combining large sized MMC agents in solution induces more noticeable effects to ECM matrix cellular response as well as volume exclusion effects

(Chen et al 2011, Magno et al 2017). If single MMC agents are unable to obtain the team's desired matrix modification for pancreatic TME simulation, we felt the combination of MMC agents in solution during gelation could provide a more potent approach to modulating the organization of engineered matrices.

4.2.3 Electrospinning for 2.5D Scaffold Models and 3D Layering

Electrospinning produces variable fiber sizes and density to create a 2.5D scaffold. Also because of the random fiber organization, different architectural designs can be created, to determine the degree of heterogeneity that is possible (Cheng et al, 2017). A 2.5D scaffold is a surface that has topography features (grooves, pores, proteins) that can be a favorable surface for cell attachment, and studies on cell interactions with different fiber organizations could give information about the effects of heterogeneous organization on cell growth and morphology (Davidson et al, 2020). However because the client requested a 3D in vitro model, other approaches were explored to incorporate the advantages of electrospinning into a 3D format.

One option to create a 3D scaffold with electrospinning was to stack electrospun scaffolds in a layer by layer approach until a 3D scaffold of significant thickness was produced as seen in (Figure 3). To have cells throughout the scaffold, cell-seeded scaffolds would be stacked in wells prior to adding cell culture medium. The 3D scaffold would likely have to be anchored to the bottom of the well in some way to prevent floating, so some sort of biocompatible adhesive would need to be used.

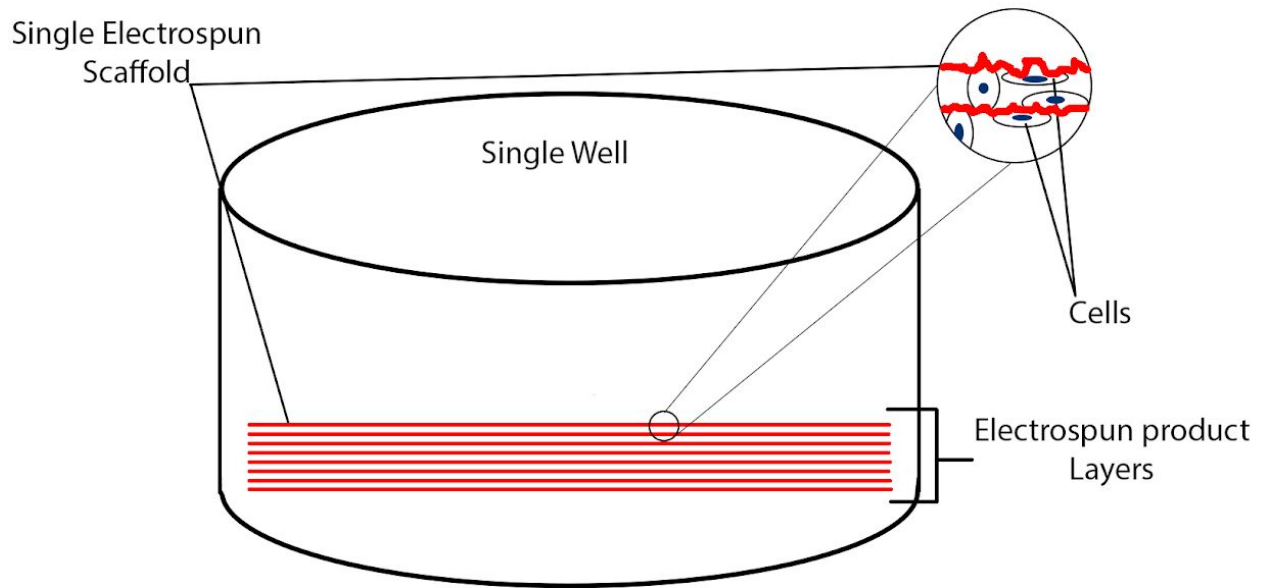


Figure 3: Concept of layering electrospun products together to create a 3D scaffold.

4.2.4 Electrospun Layering within Hydrogel

Another alternative to gain stability and an anchor point is through layering the electrospun scaffold within a hydrogel as seen in (Figure 4). Cell-seeded scaffolds would be stacked in wells, then the hydrogel solution will be added and allowed to polymerize prior to adding cell culture medium. Adjustments to this model can also be made, such as spacing of the electrospun layers, and incorporating a hydrogel with cells instead of pre-seeding the scaffolds with cells to see how cells interact with different fiber structures within the hydrogel. The hydrogel material itself can also be altered to observe different material interactions with the cells.

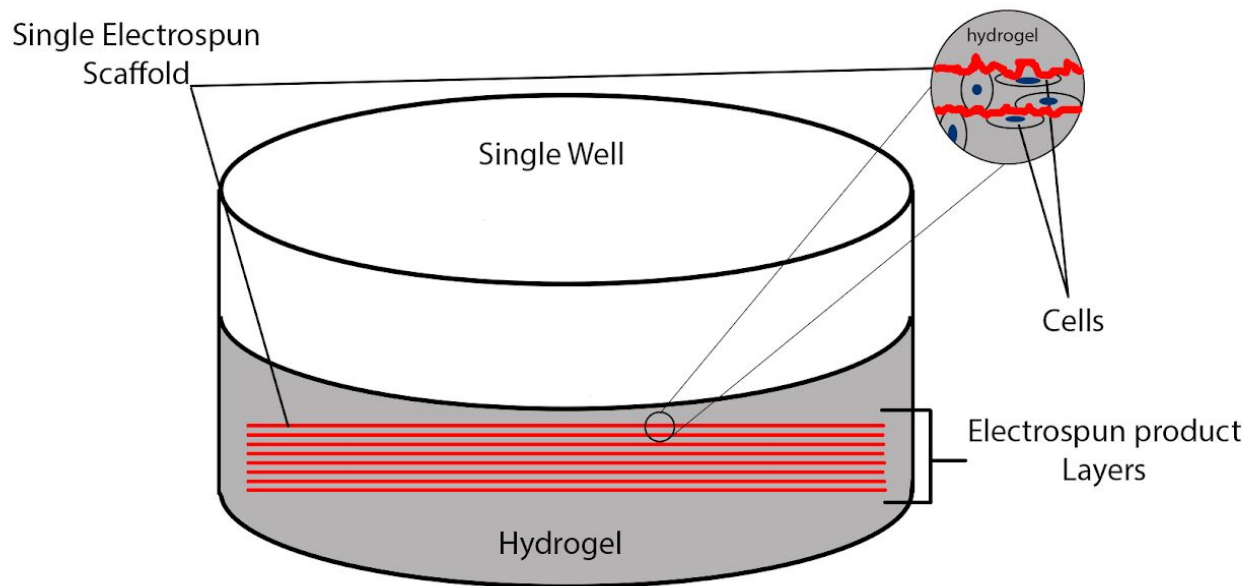


Figure 4: Concept of layering electrospun products within a hydrogel to create a 3D scaffold.

4.3 Final Design Selection

The final design integrated certain aspects of the aforementioned methods, materials, and techniques. The design base utilized ECM components: Type I collagen, decellularized porcine pancreata, and alginate for ECM reconstruction. Type I collagen is widely utilized for a variety of research settings and is generally considered the gold standard for in vitro tissue models (Sung et al, 2009, Puls et al 2017, Mason et al, 2013). The team felt collagen would provide a necessary baseline to compare with the other in vitro tissue biomaterials we chose. The team ultimately decided to use decellularized tissue and alginate. The team contacted a local slaughterhouse (Adam's Farms, Athol MA) and confirmed their screening process (Appendix A) to ensure a supply of non-contaminated porcine pancreas tissue. Furthermore, the decellularization process (Appendix B) included multiple sterilization steps to ensure the tissue

was suitable for laboratory use. Decellularized porcine pancreas provided a means for a cost-effective source of ECM components.

Based on the source of porcine pancreatic tissue, decellularization allowed for the incorporation of multiple natural ECM macromolecules in a single material ideal as an in vitro biomaterial (Sackett et al, 2018). It has also been previously utilized in studies both for fibrotic and non-fibrotic TME analysis where it was an advantageous method for scaffold fabrication (Ferreira et al, 2020, Porzionato et al, 2018). Alginate has been fabricated into a multi-layer heterogeneous scaffold utilizing a bioprinting approach (Biscaia et al, 2017), and has potential as a material for a pancreatic TME model. Ultimately, all materials have been utilized in a variety of tissue ECM models where properties such as fiber stiffness, density, or organization have been manipulated. The team felt the variety would provide more customization opportunities for the final design to provide the best possible simulation of a heterogenous, fibrotic pancreatic TME, as well as application in different organs or tissue environments for other researchers in the future.

Electrospinning and MMC were chosen over bioprinting. Although bioprinting has recently received attention for its use in tissue engineering (Miri et al, 2019), a comprehensive understanding of the tissue being modeled is needed to fabricate tissue scaffolds. Even for relatively simple tissue types, the sheer volume of cellular interactions that occur reaches staggering complexity (Bishop et al 2017). Electrospun ECM components can be utilized for topological analysis in 2D (Davidson et al, 2020, Cheng et al, 2017). Furthermore, we proposed to stack electrospun scaffolds in a layer-by-layer approach until a 3D scaffold of significant thickness is produced. This fabricated 3D scaffold could then be utilized for analysis or

combined with hydrogels in a well for more variation of scaffold spacing or cell seeding. These hydrogels themselves provided more options for controlling fiber spacing and alignment. Ficoll 70 and 400 along with PEG were introduced to the type I collagen during polymerization at varying single crowder concentrations.

5. Design Verification

In this section the team is going to test the preliminary design, the experiments were performed in MMC confocal imaging, turbidity test, and electrospinning to evaluate the potential construct of the in vitro model.

5.1 Turbidity Assay with Macromolecular Crowders

Polymerization of collagen with the chosen MMC agents was evaluated using a turbidity assay that measures the opacity of a sample at a particular wavelength. For the turbidity experiment, growth rate, lag time, and time to half maximum absorbance were evaluated as indicators of the collagen polymerization kinetics (Figure 5).

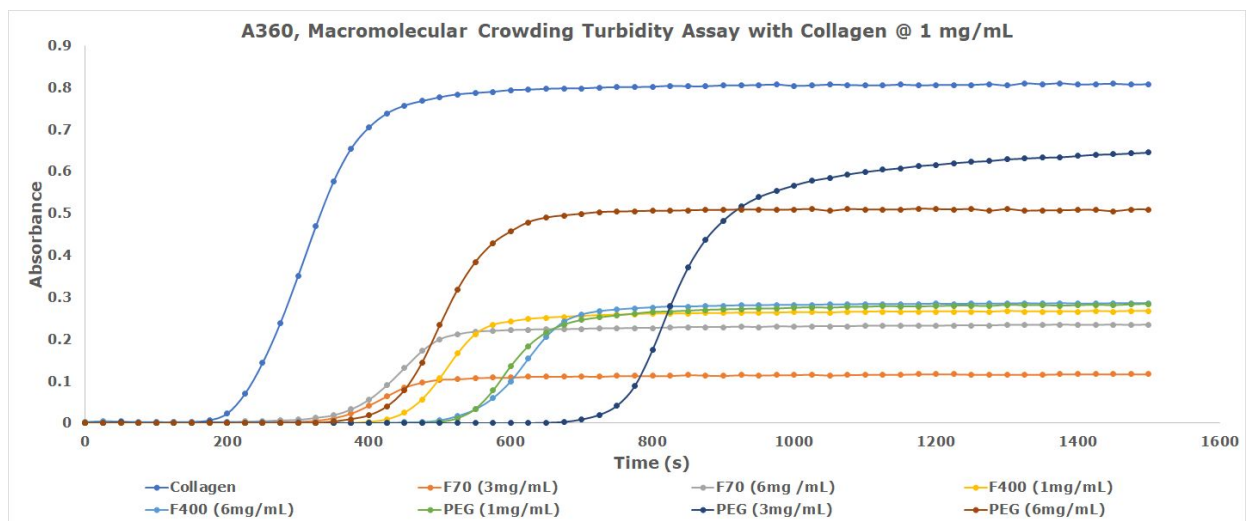


Figure 5: Turbidity assay results for type I collagen with crowding agents. N = 1, n = 3.

Table 5: Polymerization Kinetics of Collagen with Crowding Agents

Materials	Growth Rate* (Absorbance/Min)	Lag Time (Min)	Half Max (Min)
Control	4.27 ± 0.90	4.86 ± 0.96	1.46 ± 0.21
Ficoll 70 (3mg/mL)	1.11 ± 0.31	5.83 ± 0.00	1.04 ± 0.00
Ficoll 70 (6mg/mL)	2.60 ± 0.65	5.97 ± 2.10	1.18 ± 0.24
Ficoll 400 (1mg/mL)	3.46 ± 1.22	8.06 ± 0.64	0.90 ± 0.12
Ficoll 400 (6mg/mL)	3.09 ± 0.76	9.31 ± 0.24	0.97 ± 0.12
PEG (1mg/mL)	2.23 ± 0.58	14.58 ± 8.25	1.04 ± 0.00
PEG (3mg/mL)	3.52 ± 1.27	10.63 ± 2.65	1.25 ± 0.29
PEG (6mg/mL)	4.19 ± 1.56	6.88 ± 0.29	1.25 ± 0.29

Notes: N = 1, n = 3. PEG = Polyethylene Glycol, * = 10⁻⁵

The average growth rate, lag time, and time to half maximum absorbance time were calculated for each crowding condition (Table 5). There were some conditions that did not polymerize, and since only one experiment was run, no statistical analysis was performed. For most conditions, the concentration of crowders appeared to increase the maximum absorbance value (i.e., plateau), which could be an indicator of density. The presence of the crowding agents also appeared to inhibit the early stages of collagen polymerization as demonstrated by increased lag times compared to the control. However, the crowders did not appear to cause a problem for overall polymerization, since the times to half maximum absorbance for all samples were shorter than that of the collagen control.

5.2 MMC Confocal Imaging and Analysis

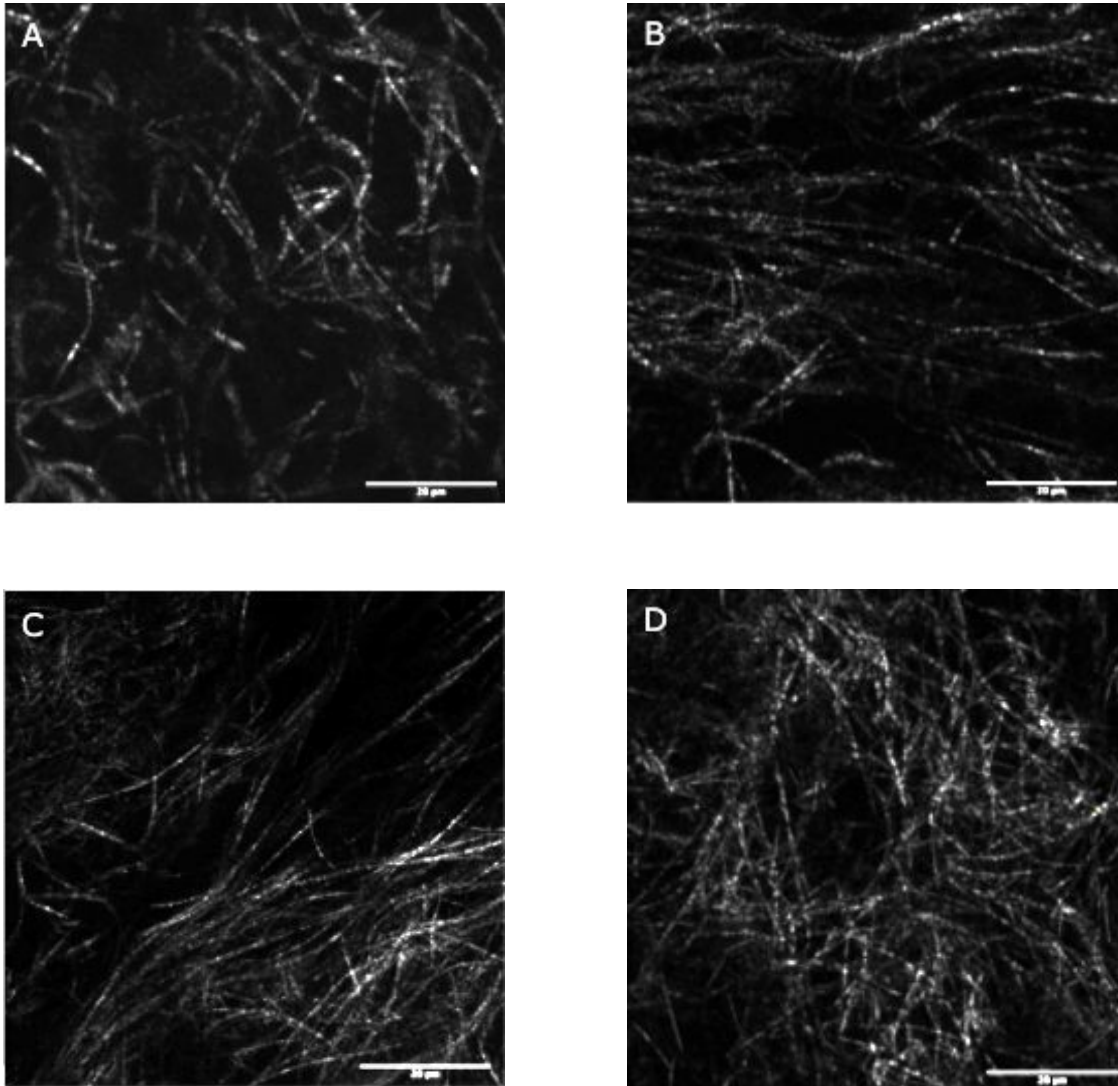


Figure 6: MMC Confocal images of type I collagen at 1 mg/mL with: **A:** no crowding agent. **B:** Ficoll 70 at 6mg/ml. **C:** with Ficoll 70 at 3mg/ml. **D:** Ficoll 400 at 1mg/ml. All images were taken with a 20x objective, scale bar is 20 microns.

To analyze the effects of MMC crowding agents on control type I collagen at a 1mg/ml concentration, confocal laser scanning microscopy (CLSM) was performed to obtain high

resolution images, and FIJI ImageJ cell analysis software (National Institutes of Health) was used to analyze images (directionality, porosity).

In the first MMC trial, the only samples that fully polymerized were the control group with no crowding agents and collagen with Ficoll 400 at 1 mg/ml, Ficoll 70 at 3mg/ml, and Ficoll 70 at 6 mg/ml (Table 6).

Table 6: Directionality of different groups of crowding agents in different concentration

	Ficoll 70 @6 mg/ml	Ficoll 70 @3 mg/ml	Ficoll 400 @1mg/ml	Col I
Direction (degree)	-6.97	30.44	-17.74	-40.34
Dispersion (degree)	13.38	20.25	31.78	20.35
GOF	0.89	0.89	0.89	0.49

(Table 6) shows the direction, dispersion degree, and goodness of fit for the directionality analysis. The direction in degree indicates the median of most fiber aligning degrees, showing the overall fiber position. The dispersion in degree indicates the distribution of fibers, the larger dispersion degree is, the more randomness the fiber is; on the other hand, smaller dispersion degree means the fibers are more aligned in the image area. GOF, the Goodness of fit line, is the linear relationship to describe the overall fiber alignment; higher GOF indicates that the line can better describe the trends of fiber alignment in the histograms below, and the lower GOF demonstrates the lower representation of the line can describe the trends.

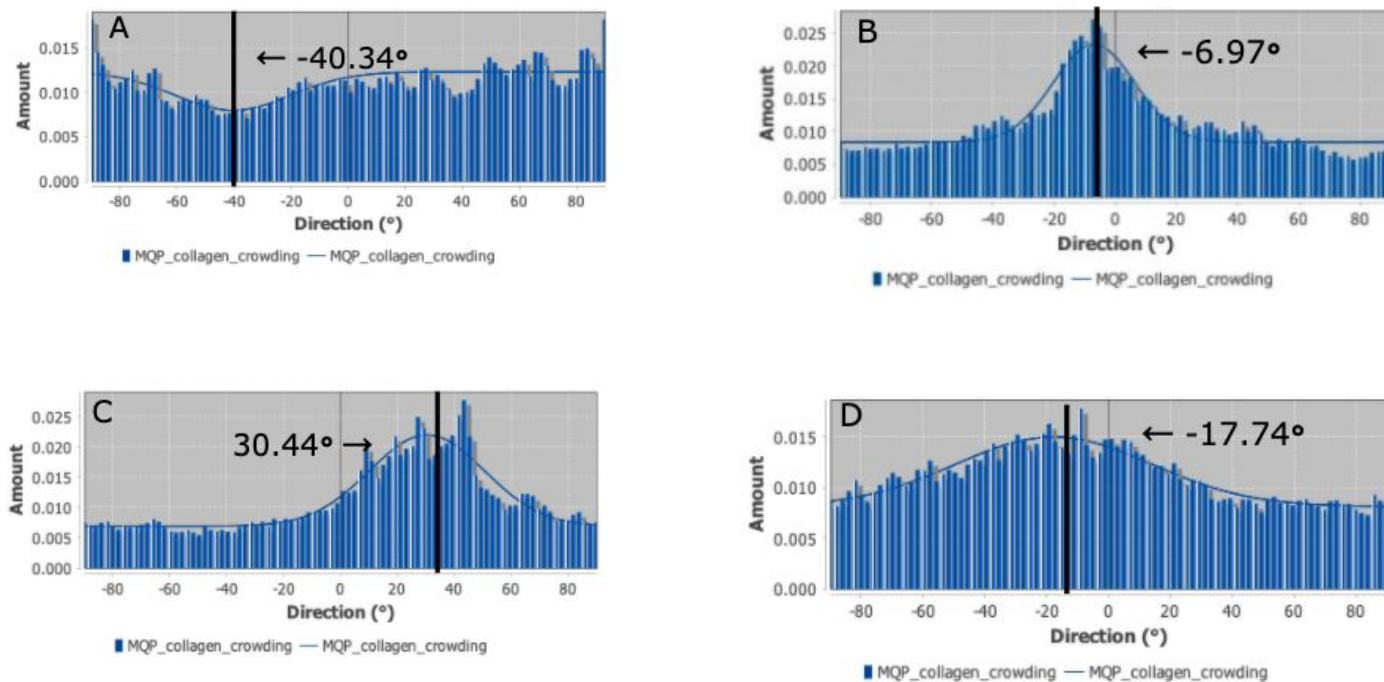
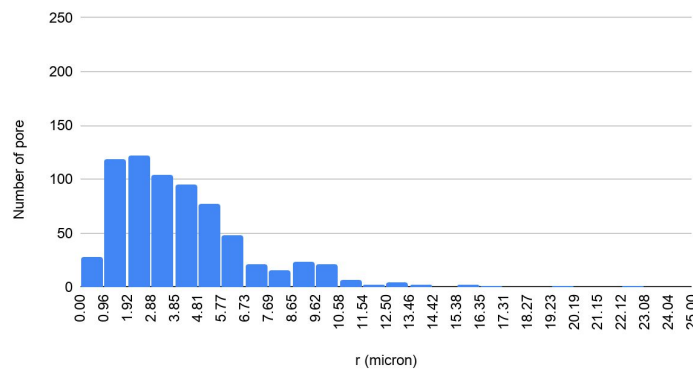


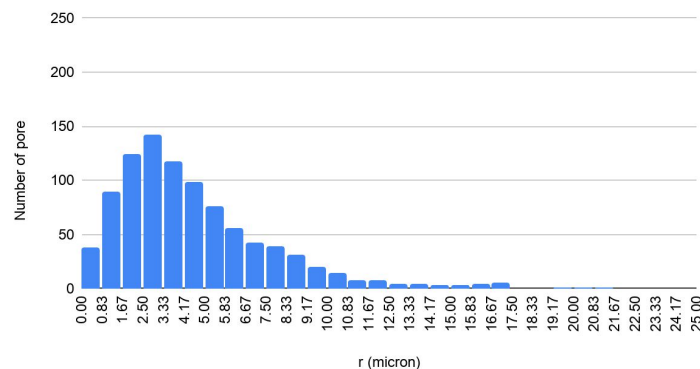
Figure 7: Directionality histograms of **A:** control type I collagen . **B:** Ficoll 70 6 mg/ml. **C:** Ficoll 70 3mg/ml. **D:** Ficoll 400 1 mg/ml.

The (Figure 7) directionality histograms summarize the fiber alignment information. Graphs with an obvious hump and sharper curves represented fibers that were more likely to be aligned to the same degree and were considered to have more orderly distribution. Graphs with flatter distribution showed that the fibers were less organized and arranged. From (Figure 7), Ficoll 70 at both concentrations showed that fibers were more aligned in the scanned area. Ficoll 400 at 1mg/ml and the control sample showed that fiber alignment was more randomized than the other two samples.

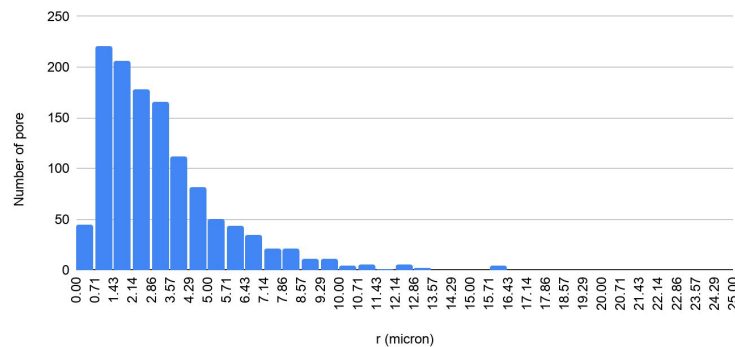
A: Histogram of pore size (Col 1)



B: Histogram of pore size (Ficoll 70 6mg/ml)



C: Histogram of pore size (Ficoll 70 3mg/ml)



D: Histogram of pore size (Ficoll 400 1mg/ml)

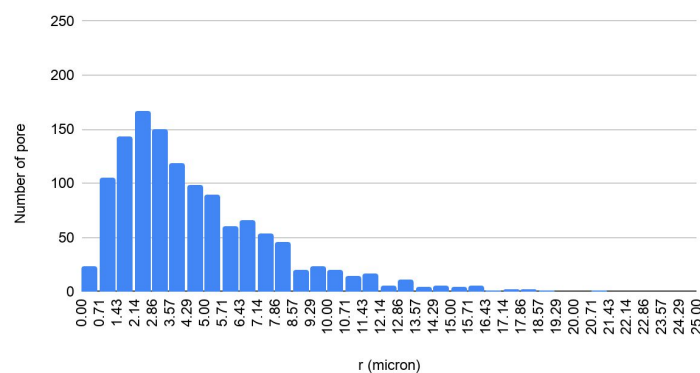


Figure 8: Histogram of pore size for **A** control collagen. **B:** Ficoll 70 at 6mg/ml. **C:** Ficoll 70 at 3mg/ml. **D:** Ficoll 400 at 1mg/ml.

Table 7: Pore analysis of different groups of crowding agents in different concentrations.

	Control	Ficoll 70 @ 6 mg/ml	Ficoll 70 @ 3 mg/ml	Ficoll 400 @ 1 mg/ml
Average Pore Size (micron)	4.21	4.59	3.28	4.66
Pore Number	695	932	1225	1260

The pore size histograms (Figure 8) summarized the porosity information about the hydrogels with some indication of fiber length. (Table 7) showed that Ficoll 70 at 3mg/ml had a high pore count with smaller pores, which suggested that Ficoll 70 3mg/ml crowded the collagen to a point where fiber length appeared to be smaller and segmented compared to other samples. Ficoll 70 at 6mg/ml had a similar distribution Ficoll 400, but Ficoll 400 had a higher pore count. The average pore size for those two conditions was similar, so Ficoll 400 may have also crowded the collagen to a higher degree. The control samples had the lowest pore count with a mid-range average pore size compared to the other samples which suggested less crowding, as expected. These data showed that the Ficoll 70 at 3mg/ml had the most aligned fibers with the highest degree of crowding (Figure 9).

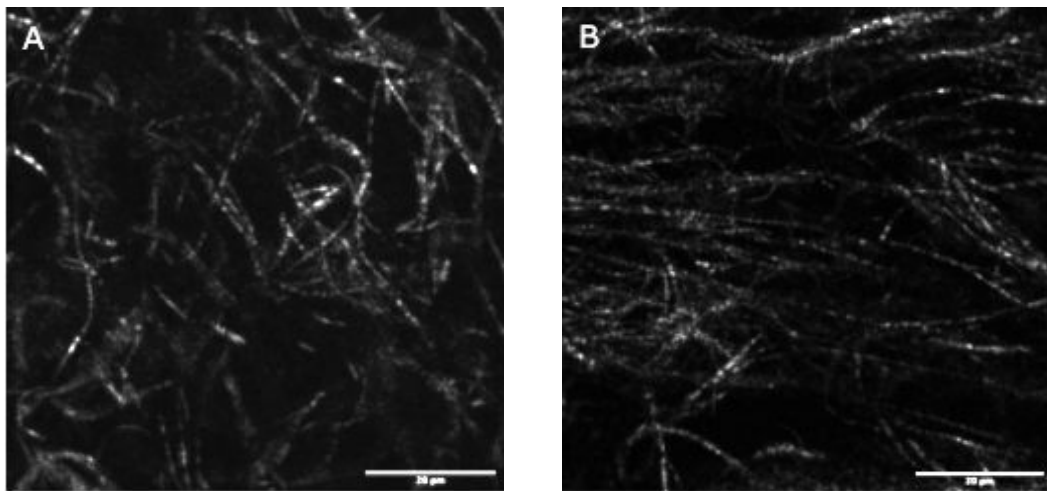


Figure 9: Confocal image of **A:** Control group and **B:** Ficoll 70 at 6 mg/ml.

Table 8: Comparison set for MMC control group and Ficoll 70 at 6mg/ml

	Control	Ficoll 70
Direction(°)	-40.34	-6.97
Dispersion(°)	20.35	13.38
Mean Pore Size(micron)	4.21	4.59
Pore Number	695	932
P-Value	0.0145	

The team compared different crowders to find the potential for introducing a higher degree of heterogeneity. The primary parameters for comparison were fiber distribution, pore size, and pore number. The team used the two-sample T-test to evaluate the significance of the difference between pore numbers in the control group and groups with MMC crowders. The smaller P-value signified higher degrees of differences in the scanned area (Table 8). From the current data, the team noted the potential use of Ficoll 70 and Ficoll 400 as crowders due to high dispersion degrees and small P values for a higher degree of difference.

5.3 Electrospinning

Initial testing of the electrospinning apparatus was performed using alginate since the decellularized ECM was not ready at the time. Collagen and gelatin were also not used due to the need for temperature control. Additional crosslinking would have also been needed for gelatin to maintain the structure at physiological temperature. Compared to collagen, alginate was a cheap

alternative that can be electrospun in large quantities with carrier polymers to form fiber-like structures. The carrier polymer that was used was polyethylene oxide (PEO). Another carrier polymer was considered, polyvinyl alcohol (PVA), however it was eliminated due to complications making the PVA solution.

To determine if the alginate (40 mg/mL), PEO (40 mg/mL), or a combination of the two (20-20 mg/mL) could form a hydrogel before electrospinning, rheological testing was performed. The shear storage modulus (G') and loss modulus (G'') was recorded for each sample (Figure 10). After 20 minutes, G' and G'' values were low for all samples and G' and G'' curves never crossed to indicate the transition from a liquid (viscous) to solid (elastic) state. This observation suggested that neither material could form a hydrogel without a crosslinker.

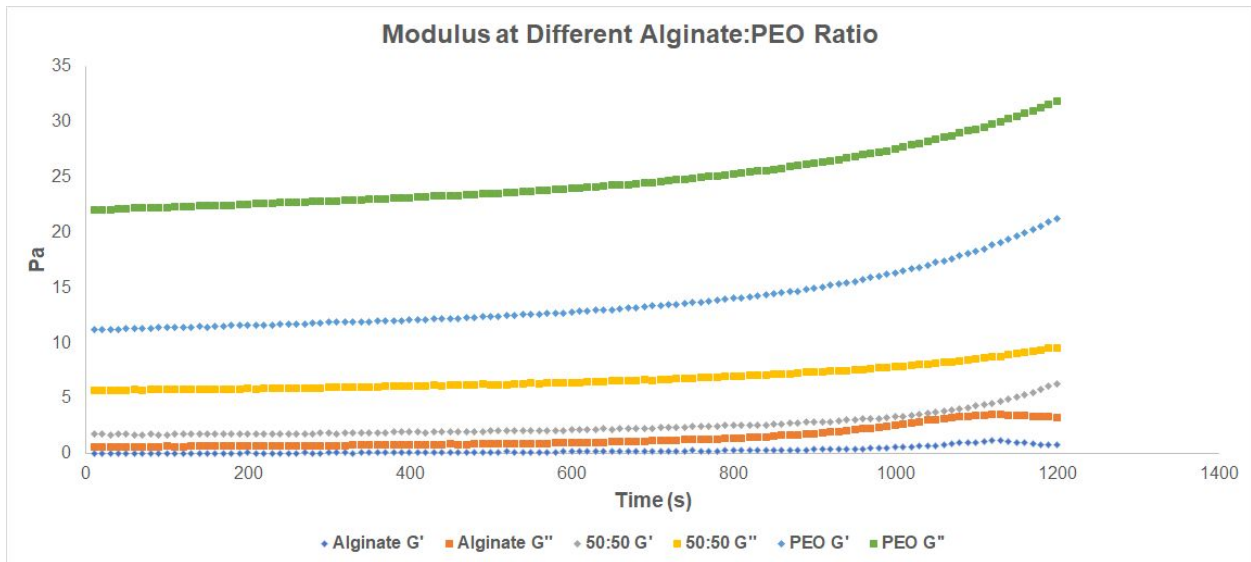


Figure 10: Shear storage and loss modulus at different alginate:PEO ratio, n = 3 for each condition.

Combinations of alginate and PEO were electrospun at different concentrations at 0.5 mL/hr. (Figure 11) shows electrospun alginate and PEO combination at concentration 20-20

mg/mL. The surface of the product was rough, and there were differences in the topography at different locations of the sample that were visible to the naked eye. A large surface area of sample was produced through the electrospinning, which meant that cutting the sheet into smaller pieces and layering them would still be a viable option. However, the sample was also very thin, so it would likely require more layers than expected to create a 3D scaffold of electrospun scaffolds to produce the in vitro model. In addition, due to the high opacity of the sample, the product could not be imaged using light or fluorescence microscopy.



Figure 11: Electrospun product of alginate and PEO at concentration 20-20 mg/mL.

6. Final Design Verification

6.1 Assessment of Objectives

6.1.1 Ease of Use

Objective 1 was that the model should be easy to handle, sterilize, and analyze for fibrotic features. The design of the model should be intuitive to all levels of researchers regardless of the experience. Since the protocols were well established, the team met the objective. The final design was produced and sterilized under the conventional laboratory conditions based on the standard of ISO 11737-2:2009, “Sterilization of medical devices”. The preparation time for decellularized ECM production took up to 2 weeks, but was consistently performed twice. For fibrotic feature analysis, the team used confocal laser scanning microscopy (CLSM) to capture images and ImageJ to analyze images. Both are reasonably accessible in research laboratory spaces.

6.1.2 Heterogeneously Organized

Objective 2 was that the model should be heterogeneously organized with varying degrees of ECM density and fiber alignment. The team conducted the MMC experiment to see if the crowding agent affected matrix properties, and the result showed the crowding agents have the potential to alter the fiber alignment and porosity within the matrices. The objective is not completed, because further testing of additional crowding (single and multiple agents) with

chosen materials could not be performed due to COVID-19. However, the team gained early insight into which crowding agents could potentially be used to achieve heterogeneous fibril networks.

6.1.3 In Vivo Characteristics

Objective 3 was the model should replicate in vivo characteristics of fibrotic tissue. The team should use combinations of materials and approaches to produce the model. The model should mimic the in vivo tissue including similar macromolecule composition and mechanical properties. The team didn't complete this objective because testing for verification of material and approaches was not performed due to COVID-19. The team has the raw material of decellularized ECM ready so future testing can be performed with this potential material. The in vitro model will have to be tested for cytotoxicity based on the ISO standard 10993-5:2009 "Tests for in vitro cytotoxicity", for biocompatibility based on ASTM standard F2739-16 "Standard Guide for Quantifying Cell Viability within Biomaterial Scaffolds".

6.1.4 Reproducible

This objective 4 the model fabrication and related analyses should be reproducible across multiple users. The team didn't complete this objective because the model was not accomplished. The team conducted the protocols of experiments so other project teams can follow cohesive steps to complete the model.

6.1.5 Cost Effective

Objective 5 was that the team should balance the cost and efficiency throughout the design process. The team completed the objective by limiting the total cost to be under \$1000. The team chose to use cheaper fresh pig pancreas instead of purchasing more expensive native collagen I. The team utilized the available equipment in the laboratory including the tissue homogenizer and electrospinner. The team also purchased a small amount of crowding agents based on our projected needs to prevent excessive spending.

6.2 Summary of Experimental Analysis

6.2.1 Means

Upon the completion of design objectives, the team analyzed various means of achieving the listed functions. The functions and their corresponding means are as follows (Table 9).

Table 9: Functions and Means of Design Requirements

Function	Mean 1	Mean 2
Simulate in vivo pancreatic ECM stiffness, interstitial spacing, and fiber organization	Varying the concentration of ECM component hydrogelled (1mg/ml, 3mg/ml, 4.5 mg/ml)	Crowding microenvironment with separate and combined agents (Ficoll 400, Ficoll 70, PEG)
Model for both 2D and 3D fibrotic pathology analysis	Macromolecular crowding cocktails for hydrogels in 2D	Stacking of electrospun scaffolds for 3D modeling
Retain physiological conditions for accurate modeling	ECM components derived or observed naturally (collagen I, decellularized pig pancreas)	Multiple sterilization steps during matrix construction to ensure decontamination of materials, performed in biosafety cabinet

To achieve the first objective of simulating the in vivo pancreatic ECM stiffness, interstitial spacing, and fiber organization, ECM components as well as MMC agents will be mixed in solution at varying concentrations to simulate the tissue ECM properties. The next function is the ability to be utilized for both 2D and 3D fibrotic pathological modeling. The means for this function will be obtained by using MMC crowding agents for 2D analysis, and we propose to stack 2D electrospun scaffolds to fabricate a 3D model. The final function our design should have is the retention of physiological conditions for accurate modeling. The means for this function include deriving ECM components from decellularized porcine pancreata and using naturally occurring type I collagen ECM components for scaffold fabrication. In addition, multiple sterilization steps including protocol execution in a biosafety cabinet will be implemented to ensure the materials are decontaminated and sterile.

6.2.2 Decellularization of Pancreas Tissue

Porcine pancreata sourced from a local slaughterhouse (Adam's Farms, Athol MA) was processed according to an established protocol (Rice et al, 2017). The tissue was homogenized, decellularized, treated with antibiotics, and lyophilized (Sackett et al, 2018). To prepare samples, lyophilized ECM was solubilized in hydrochloric acid containing pepsin and exposed to neutralization buffers to promote polymerization (Freytes et al, 2008). Appendix B contains the detailed procedure of decellularization and (Figure 12) is a schematics of the process.

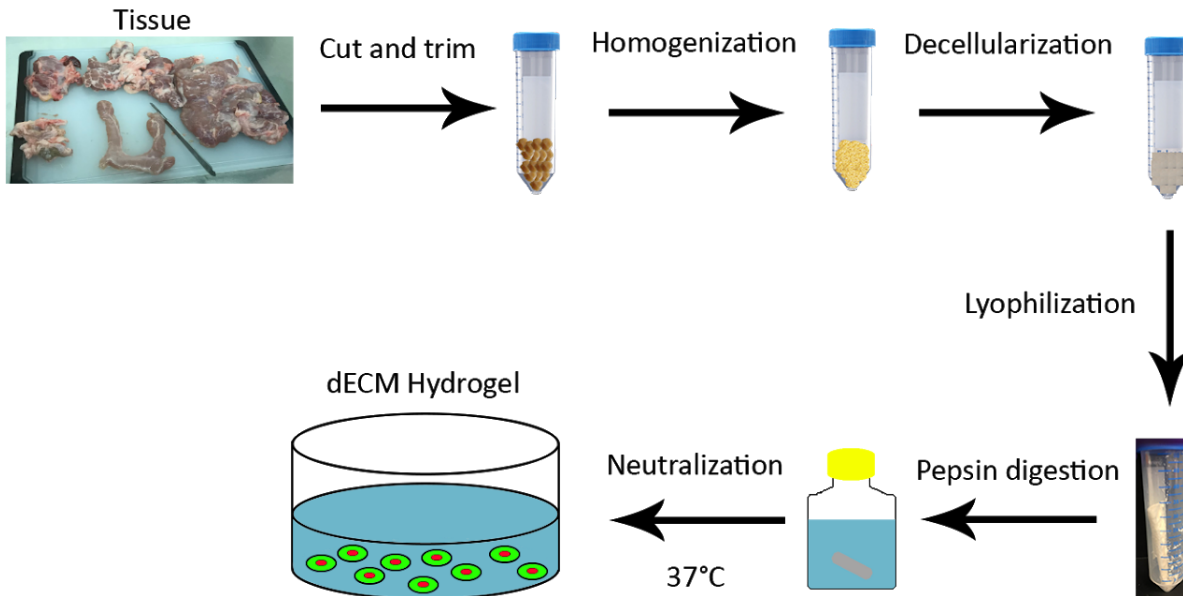


Figure 12: Schematic representation of decellularized ECM hydrogel process.

6.2.3 Preparation of Collagen Hydrogel with Single Crowding Agents

Established protocols to prepare collagen hydrogels were used and adjusted to include crowding agents in the neutralization buffers. Type I collagen (1 mg/mL) was combined with single solutions of common crowding agents: Ficoll 70 (abcam, ab146571) and 400 (Sigma

Aldrich, F9378); Polyethylene Glycol (PEG) (Sigma Aldrich, 89510) in phosphate buffered saline to achieve a final concentration of crowder (1-, 3-, and 6 mg/mL). Samples were prepared for turbidity analysis and confocal laser scanning microscopy (CLSM). Appendix C contains the detailed procedure of the hydrogel formation with single crowding agents and the plate layout used in testing.

6.2.3 Turbidity Analysis of Hydrogels with Single Crowders

Condition groups from Ficoll 70, Ficoll 400, and PEG were added to neutralized type I collagen (1 mg/mL) to achieve a final crowder concentration of 1 mg/mL, 3 mg/mL and 6 mg/mL (n=9). Additionally, a control group of 1 mg/mL of type I collagen with no crowder was included.

For turbidity analysis, absorbance readings were measured using a spectrophotometer plate reader at 360 nm and 405 nm (37°C) for one hour. Samples of 100 µL of the final solutions of collagen and crowder agent mixture were added in triplicate to a 96 well plate on ice to prevent spontaneous polymerization.

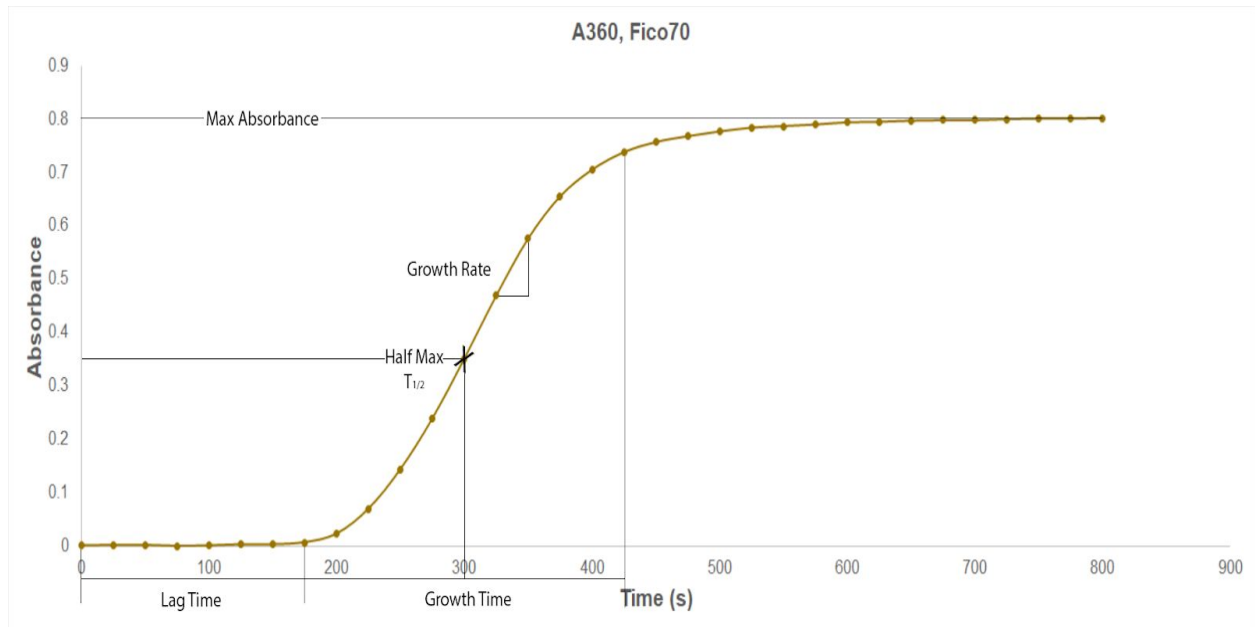


Figure 13: Example of a turbidity graph with label parameters.

(Figure 13) shows the parameters of interest used to compare samples when using a turbidity assay to monitor polymerization kinetics. The growth rate was determined using the linear portion of the curve where a linear fit was performed to obtain the slope as a measure of growth rate. The lag time was recorded as the time polymerization started to occur, which is the x-intercept of the slope-intercept equation used for growth rate. The half maximum time was recorded as half of the time it takes to reach half of the max absorbance. This value was also calculated using the slope-intercept equation used for growth rate.

6.2.4 MMC Confocal Imaging and Analysis

For CLSM studies, the team created six sample groups with different crowders in different concentrations and one control group containing only pure collagen without crowders.

The original experiment included Ficoll 70 and Ficoll 400 with each crowder at 1 mg/mL, 3 mg/mL, and 6 mg/mL final concentration in the base type I collagen formulation (1 mg/mL). Only three experimental groups polymerized in the first trial, so images were only taken for Ficoll 70 at 3 mg/mL, Ficoll 70 at 6 mg/mL, Ficoll 400 at 1 mg/mL and the control group. During image capture, the samples were placed on a glass-bottom petri dish, and PBS was added to prevent dehydration. Images were taken with a 20x oil objective on a Leica Point Scanning Confocal SP5 Microscope. The collagen was not stained so the images were taken in reflectance mode to capture backscattered light from the collagen fibers. Images were analyzed using FIJI ImageJ (National Institutes of Health).

To satisfy the objective of assessing heterogeneity, the team selected the parameters to determine the degree of heterogeneity to be fiber directionality, pore size and pore number. Appendix D contains a detailed protocol about using FIJI ImageJ to find fiber directionality and pore data for future analysis.

6.2.5 Preparation of Alginate/PEO with Electrospinning

A combination of alginate and polyethylene oxide (PEO) with 1% Triton X-100 at concentrations 28-12-, 20-20-, and 12-28 mg/mL were used for electrospinning. Samples were run at 0.5 mL/hr with a 21 gauge blunt needle. Voltage was adjusted between 6-10 volts depending on the sample, and the collection mesh (tin foil) was placed (4, 8, 12) inches away from the needle. A breakdown of these parameters can be found in (Table 10), and a more detailed protocol can be found in Appendix E.

Table 10: Parameters on how electrospinning was run using Alginate/PEO solutions.

Fixed Parameters	Needle size	Spinning Rate	Voltage
		21G	0.5 mL/hr
Changing Parameters			
Alginate/PEO Concentration	28/12 mg/mL	20/20 mg/mL	12/28 mg/mL
Distance	4 inches	8 inches	12 inches

6.3 Impact of Final design

6.3.1 Economics

There is an economic opportunity that exists for the development of a model for a fibrotic disease model. The design and development of a pancreatic microenvironment with controllable fibril directionality, alignment, and porosity is beneficial for researchers and addressing industry gaps. The utilization of cost effective modeling techniques (i.e., MMC and electrospinning) and ECM alternatives model can reduce the significant material and design costs. The success of designing a heterogeneous in vitro fibrosis model capable of producing controllable fibril phenomena could be used for testing varying scaffolds and techniques.

6.3.2 Environmental Impact

The fabrication of these engineered fibrotic matrices would have a minimal impact on the environment. The largest sustainability factor comes from the sourcing of porcine pancreata for

decellularization and commercial sourcing of other materials according to their respective procedures. By sourcing from USDA approved slaughterhouses where pig organs are screened and gathered for human consumption, the model does not excessively take from or impact the environment. Furthermore, other materials used (collagen, macromolecular crowders) have detailed procedures for safe handling and disposal and are not expected to harm or contaminate the environment.

6.3.3 Societal Impact

Successful development and production of an in vitro engineered fibrotic microenvironment model with heterogeneous spatial organization holds potential for medical benefits in society. Utilization of such a model for testing of therapeutic targets of pancreatic cancer would help in the isolation and identification of potential biomarkers for the development of targeted therapies. By controlling the fiber density, interstitial spacing, and organization of the model, researchers could target specific TME properties like low vs high fiber concentration and observe its effect, if at all, on tumorigenesis to further validate potential therapies using a more predictive in vitro model.

6.3.4 Political Ramifications

Currently in the United States, there is a high demand for improvement in cancer research and care. Disease modeling approaches have received more attention in the medical field because of the ability to better understand in vivo processes. There is also a growing need to combat fibrotic diseases that are among the leading causes of death in the United States. Therefore, there are no anticipated political ramifications.

6.3.5 Ethical Concerns

There are minimal ethical concerns regarding design and function of this system. Like current models used, the development of this system uses *in vitro* testing methods. This allows for experimentation to be conducted outside of living organisms before pursuing any potential animal studies and reduces overall dependence on animal models. By using a variety of scaffold materials and modification techniques, a successful model will be able to mimic the fibrotic microenvironment of the pancreas. Our approach has limited ethical concerns because animal models are not being used. However, this does not entirely eliminate the incorporation of animal subjects for future testing. Additionally, the project makes use of animal sourced materials such as porcine derived ECM and bovine type I collagen. However, the *in vitro* fibrosis model does not have to solely rely on animal sourced materials, which would lower ethical concerns regarding the testing procedure.

6.3.6 Health and Safety Issues

The overall design of our heterogeneous fibrotic system involves the understanding of pathological processes occurring *in vivo* with pancreatic cancer and fibrotic disease. The processes and experiments related to this design were performed according to Biosafety Level 2 safety protocols in a laboratory at WPI. All sanitation procedures and waste disposal were performed according to the regulations outlined by WPI Environmental Health and Safety. Continued use of sterile equipment and biosafety cabinets will reduce production of byproducts and contamination to users. Adherence to protocols will decrease concerns related to health and safety.

6.3.7 Manufacturability

The production of an in vitro fibrotic model with controlled heterogeneities consists of material procuring and fabrications. Materials such as bovine derived type I collagen are costly, available online for approximately \$200 at 3 mg/mL. However, materials can be purchased from many commercially available sources. The use of decellularized ECM increases processing time considerably and the overall yield can be low. The fabrication of scaffolds takes upwards of 6 hours using MMC and or electrospinning. However, the matrix materials and reagents do not require special handling for short- or long-term storage. Overall, the manufacturing process is reasonable for the final design of this fibrotic model.

6.3.8 Sustainability

Tissue parts that would normally be disposed of by the slaughterhouse could be decellularized and become an available resource. The fabrication of hydrogels does not require excessive materials or resources. There is no environmental harm as the reagents such as collagen, decellularized ECM, Milli-Q water, and crowding agents will either be transferred to a chemical waste container or bleached to be safely discarded. The only concern is the amount of energy electrospinning would use as slower rates of spinning will keep the machine on longer.

7. Discussion

It has been established that there is a relationship between tumor metastasis-related signaling and the heterogeneity and fiber composition that comes with fibrotic tissue. After going through the design process, the team decided to pursue macromolecular crowding (MMC) and electrospinning with decellularized pancreatic ECM as possible ways to engineer an ECM with heterogeneity.

With the literature showing the MMC process could achieve the desired matrix modification, the experiment MMC agents group shows the significant difference compared to the control group (Zeiger et al, 2012). Further testing with other biomaterials can be processed to satisfy the requirement to mimic the real pancreatic environment. However, the current images analysis result may not fully represent the experimental group result. The team completed one sample testing, the small number of images has limited the representativeness of the actual degree of heterogeneity in the scaffold. The team aims to increase the sample size of images as well as taking images in multiple locations of each set to compare the microstructure for a more accurate assessment of heterogeneity. The team also aims to perform experiments with a combination of different MMC crowders that the combinations might induce a higher degree of heterogeneity which the team is looking for.

The turbidity test suggests that the MMC crowders might affect the gel polymerization, since in the early stage of collagen polymerization, the lag time appeared to increase when the agent concentration increased compared to the collagen control. However, the overall polymerization time is suitable for the team's needs. The team aims to repeat the turbidity test

with collagen groups, and new tests with engineered decellularized ECM should be completed in order to measure the actual polymerization time.

Electrospinning, as another potential method to build up the in vitro model, has shown some degree of satisfaction towards the goal of the team. From the literature, the technique is able to produce random fiber distribution, which induces the degree of heterogeneity. The team completed the initial test of electrospinning with alginate and PEO, the final product has obvious visual differences in topography at different locations of the sample, which gives credits in altering heterogeneity of the microenvironment. Since alginate is only one of the potential materials to use in electrospinning, the team also aims to use the decellularized ECM and collagen as their similar properties to the actual pancreatic tissue.

Based on the results from the early electrospinning experiment, the opacity of the material might become a problem for further analysis. The team also considers stiffness as one parameter to determine the tumor model environment according to the literature, so the team aims to use the atomic force microscopy (AFM) for fiber stiffness analysis and the scanning electron microscopy for microstructural analysis. In addition to the pre-existing material, the spun material might be effective when incorporated into the hydrogel to create a higher degree of heterogeneity in the 3D scaffold.

Overall reflecting on the established design objectives, the team achieved Objectives 1, 2, and 5 to varying degrees. Models were created and analyzed for fibril microstructure (Objective 1). Current image analysis provided insight into appropriate metrics on which heterogeneity could be assessed. MMC demonstrated potential to alter ECM microstructure with single agents. These observations showed progress toward achieving Objective 2 even though the objective

was not fully met. The team also met Objective 5 by staying under budget at \$700. Objectives 3 and 4 were not met due to the team's inability to continue experimental testing due to COVID-19 and the inability to access the research laboratory.

8. Conclusion

The main objective of this project was to design an in vitro fibrosis model to capture the pancreatic microenvironment. To understand fibrotic phenomena and the progression to a carcinogenic environment, fibrotic elements such as fibril alignment and density were sought to be controlled. After conducting extensive research and testing with various biomaterials which possessed unique properties in addition to ECM modification techniques, MMC and electrospinning was chosen for the final design because it demonstrated the most applicable modeling abilities. Additionally, decellularized ECM was determined to be the most suitable material for fulfilling the goals of the project. Fibril materials were successfully produced with a variety of MMC agents and PEO/alginate solution for electrospinning. The high resolution confocal images of the crowded hydrogels provided insight on the potential for heterogeneity based on fibril alignment.

For future recommendations to meet project needs and requirements, the team devised suggestions to improve the experimentation and analysis of the study. Polymerization for some materials may be hindered due to improper mixing of crowding agents. Therefore, additional turbidity tests should be done with the ECM and other materials to have more insight of gelling capabilities. Further imaging must be completed with AFM and scanning electron microscopy (SEM) to assess the fibril alignment and density of sample materials. There are currently limited photos due to the limited quantity of samples and variety of samples. A combination of crowding agents, crowder cocktails, might be helpful to achieve a higher degree of heterogeneity. This would allow for more differences in volume exclusion.

Additionally, future testing for this project should include mechanical strength testing of the scaffolds using the rheometer as originally planned. This would determine whether the fibril networks created exhibit the varied stiffness ranges of 1 kPa to 4 kPa resembling healthy and cancerous pancreatic tissue. Such testing would further satisfy design objectives for a fully functional model.

Further research into potential applications outside of pancreatic cancer to the fabrication design of the fibrosis model should be considered. Specifically, completing investigations into the fibrotic make up and mechanical properties of fibrotic tissue in other organs. Expanding parameters of related design matrices and analysis may shed light on the potential of different materials other than ECM.

References

“Pancreatic Cancer - Statistics,” Cancer.Net, 10-Apr-2019. [Online]. Available: <https://www.cancer.net/cancer-types/pancreatic-cancer/statistics>. [Accessed: Dec-2020].

T. Andersen, P. Auk-Emblem, and M. Dornish, "3D Cell Culture in Alginate Hydrogels," (in eng), *Microarrays (Basel)*, vol. 4, no. 2, pp. 133-161, 2015, doi: 10.3390/microarrays4020133.

S. Biscaia et al., "Development of Heterogeneous Structures with Polycaprolactone-Alginate Using a New 3D Printing System – BioMEDbeta: Design and Processing," *Procedia Manufacturing*, vol. 12, pp. 113-119, 2017/01/01/ 2017, doi: <https://doi.org/10.1016/j.promfg.2017.08.015>.

E. S. Bishop et al., "3-D bioprinting technologies in tissue engineering and regenerative medicine: Current and future trends," (in eng), *Genes Dis*, vol. 4, no. 4, pp. 185-195, Dec 2017, doi: 10.1016/j.gendis.2017.10.002.

C. Bonnans, J. Chou, and Z. Werb, “Remodelling the extracellular matrix in development and disease,” *Nature reviews. Molecular cell biology*, Dec-2014. doi: 10.1038/nrm3904

F. Bösch, K. Bruewer, M. D'Anastasi, H. Ilhan, T. Knoesel, S. Pratschke, M. Thomas, M. Rentsch, M. Guba, J. Werner, and M. K. Angele, “Neuroendocrine tumors of the small intestine causing a desmoplastic reaction of the mesentery are a more aggressive cohort,” *Surgery*, 31-Jul-2018. <https://doi.org/10.1016/j.surg.2018.06.026>

K. H. Bouhadir, K. Y. Lee, E. Alsberg, K. L. Damm, K. W. Anderson, and D. J. Mooney, "Degradation of partially oxidized alginate and its potential application for tissue engineering," (in eng), *Biotechnol Prog*, vol. 17, no. 5, pp. 945-50, Sep-Oct 2001, doi: 10.1021/bp010070p.

C. Chen, F. Loe, A. Blocki, Y. Peng, and M. Raghunath, "Applying macromolecular crowding to enhance extracellular matrix deposition and its remodeling in vitro for tissue engineering and cell-based therapies," (in eng), *Adv Drug Deliv Rev*, vol. 63, no. 4-5, pp. 277-90, Apr 30 2011, doi: 10.1016/j.addr.2011.03.003.

F.-M. Chen and X. Liu, "Advancing biomaterials of human origin for tissue engineering," (in eng), *Prog Polym Sci*, vol. 53, pp. 86-168, 2016, doi: 10.1016/j.progpolymsci.2015.02.004.

R. Chen, L. Huang, and K. Hu, “Natural products remodel cancer-associated fibroblasts in desmoplastic tumors,” *Acta Pharmaceutica Sinica B*, 19-Apr-2020. <https://doi.org/10.1016/j.apsb.2020.04.005>

J. Cheng, Y. Jun, J. Qin, and S. H. Lee, "Electrospinning versus microfluidic spinning of functional fibers for biomedical applications," (in eng), *Biomaterials*, vol. 114, pp. 121-143, Jan 2017, doi: 10.1016/j.biomaterials.2016.10.040.

I. K. Choi, R. Strauss, M. Richter, C. O. Yun, and A. Lieber, "Strategies to increase drug penetration in solid tumors," (in eng), *Front Oncol*, vol. 3, p. 193, 2013, doi: 10.3389/fonc.2013.00193.

M. D. Davidson, J. A. Burdick, and R. G. Wells, "Engineered Biomaterial Platforms to Study Fibrosis," *Advanced Healthcare Materials*, vol. 9, no. 8, p. 1901682, 2020/04/01 2020, doi: 10.1002/adhm.201901682.

B. Dhandayuthapani, Y. Yoshida, T. Maekawa, and D. S. Kumar, "Polymeric Biomaterials for Tissue Engineering Applications 2011," - *International Journal of Polymer Science*, vol. 2011, p. 19, 2011, Art no. 290602, doi: - 10.1155/2011/290602.

P. C. Dingal et al., "Fractal heterogeneity in minimal matrix models of scars modulates stiff-niche stem-cell responses via nuclear exit of a mechanorepressor," (in eng), *Nat Mater*, vol. 14, no. 9, pp. 951-60, Sep 2015, doi: 10.1038/nmat4350.

"F. Genten, "P12e_005_pancreás endocrine Langerhans_endocrine pancreas_Anguilla anguilla," Flickr.Net, 07-Mar-2016. "

Y. Fang and R. M. Eglen, "Three-Dimensional Cell Cultures in Drug Discovery and Development," (in eng), *SLAS Discov*, vol. 22, no. 5, pp. 456-472, 2017, doi: 10.1177/1087057117696795.

M. Feig, I. Yu, P.-h. Wang, G. Nawrocki, and Y. Sugita, "Crowding in Cellular Environments at an Atomistic Level from Computer Simulations," *The Journal of Physical Chemistry B*, vol. 121, no. 34, pp. 8009-8025, 2017/08/31 2017, doi: 10.1021/acs.jpcc.7b03570.

M. E. Feigin and D. A. Tuveson, "Challenges and Opportunities in Modeling Pancreatic Cancer," (in eng), *Cold Spring Harb Symp Quant Biol*, vol. 81, pp. 231-235, 2016, doi: 10.1101/sqb.2016.81.031104.

J. Feng et al., "Stiffness heterogeneity-induced double-edged sword behaviors of carcinoma-associated fibroblasts in antitumor therapy," *Science China Materials*, vol. 62, no. 6, pp. 873-884, 2019/06/01 2019, doi: 10.1007/s40843-018-9383-3.

L. P. Ferreira, V. M. Gaspar, and J. F. Mano, "Decellularized Extracellular Matrix for Bioengineering Physiomimetic 3D in Vitro Tumor Models," *Trends in Biotechnology*, 2020/05/13/ 2020, doi: <https://doi.org/10.1016/j.tibtech.2020.04.006>.

D. O. Freytes, J. Martin, S. S. Velankar, A. S. Lee, and S. F. Badylak, "Preparation and rheological characterization of a gel form of the porcine urinary bladder matrix," *Biomaterials*,

vol. 29, no. 11, pp. 1630-1637, 2008/04/01/ 2008, doi: <https://doi.org/10.1016/j.biomaterials.2007.12.014>.

T. Garg, "Scaffold: Tissue engineering and regenerative medicine," *International Research Journal of Pharmacy*, vol. 2, 12/03 2011.

C. Gazia, M. Gaffley, A. Asthana, D. Chaimov, and G. Orlando, "65 - Scaffolds for pancreatic tissue engineering" in *Handbook of Tissue Engineering Scaffolds: Volume Two*, M. Mozafari, F. Sefat, and A. Atala Eds.: Woodhead Publishing, 2019, pp. 765-786. <https://doi.org/10.1016/B978-0-08-102561-1.00032-4>

X. Ge, D. Luo, and J. Xu, "Cell-Free Protein Expression under Macromolecular Crowding Conditions," *PLOS ONE*, vol. 6, no. 12, p. e28707, 2011, doi: 10.1371/journal.pone.0028707.

A. Gershenson and L. M. Gierasch, "Protein folding in the cell: challenges and progress," (in eng), *Curr Opin Struct Biol*, vol. 21, no. 1, pp. 32-41, Feb 2011, doi: 10.1016/j.sbi.2010.11.001.

D. Gnutt, M. Gao, O. Brylski, M. Heyden, and S. Ebbinghaus, "Excluded-Volume Effects in Living Cells," *Angewandte Chemie International Edition*, vol. 54, no. 8, pp. 2548-2551, 2015/02/16 2015, doi: 10.1002/anie.201409847.

L. Gu and D. J. Mooney, "Biomaterials and emerging anticancer therapeutics: engineering the microenvironment," *Nature Reviews Cancer*, vol. 16, no. 1, pp. 56-66, 2016/01/01 2016, doi: 10.1038/nrc.2015.3.

J. Herrera, C. A. Henke, and P. B. Bitterman, "Extracellular matrix as a driver of progressive fibrosis," *The Journal of Clinical Investigation*, 02-Jan-2018. DOI: 10.1172/JCI93557

B. Hinz, "Myofibroblasts," *Experimental Eye Research*, vol. 142, pp. 56-70, 2016/01/01/ 2016, doi: <https://doi.org/10.1016/j.exer.2015.07.009>.

D. W. Hutmacher, "Biomaterials offer cancer research the third dimension," *Nature Materials*, vol. 9, no. 2, pp. 90-93, 2010/02/01 2010, doi: 10.1038/nmat2619.

I. Jun, H.-S. Han, J. R. Edwards, and H. Jeon, "Electrospun Fibrous Scaffolds for Tissue Engineering: Viewpoints on Architecture and Fabrication," (in eng), *Int J Mol Sci*, vol. 19, no. 3, p. 745, 2018, doi: 10.3390/ijms19030745.

M. E. Katt, A. L. Placone, A. D. Wong, Z. S. Xu, and P. C. Searson, "In Vitro Tumor Models: Advantages, Disadvantages, Variables, and Selecting the Right Platform," (in English), *Frontiers in Bioengineering and Biotechnology*, Review vol. 4, no. 12, 2016-February-12 2016, doi: 10.3389/fbioe.2016.00012.

M. E. Klontzas, H. Drissi, and A. Mantalaris, "The Use of Alginate Hydrogels for the Culture of Mesenchymal Stem Cells (MSCs): In Vitro and In Vivo Paradigms," *IntechOpen*, July 24th 2019 2019, doi: 10.5772/intechopen.88020.

- N. Kumar, H. Joisher, and A. Ganguly, "Polymeric Scaffolds for Pancreatic Tissue Engineering: A Review," (in eng), *Rev Diabet Stud*, vol. 14, no. 4, pp. 334-353, Winter 2018, doi: 10.1900/RDS.2017.14.334.
- B. S. Kwak et al., "In vitro 3D skin model using gelatin methacrylate hydrogel," *Journal of Industrial and Engineering Chemistry*, vol. 66, pp. 254-261, 2018/10/25/ 2018, doi: <https://doi.org/10.1016/j.jiec.2018.05.037>.
- N. Kramer, A. Walzl, C. Unger, M. Rosner, G. Krupitza, M. Hengstschläger, and H. Dolznig, "In vitro cell migration and invasion assays," *Mutation research*, vol. 752, no. 3, pp. 10-24, 2013, doi:10.1016/j.mrrev.2012.08.001.
- S. Lamouille, J. Xu, and R. Derynck, "Molecular mechanisms of epithelial–mesenchymal transition," *Nature Reviews Molecular Cell Biology*, vol. 15, no. 3, pp. 178-196, 2014/03/01 2014, doi: 10.1038/nrm3758.
- H.-Y. Liu, M. Korc, and C.-C. Lin, "Biomimetic and enzyme-responsive dynamic hydrogels for studying cell-matrix interactions in pancreatic ductal adenocarcinoma," *Biomaterials*, vol. 160, pp. 24-36, 2018/04/01/ 2018, doi: <https://doi.org/10.1016/j.biomaterials.2018.01.012>.
- D. Loessner et al., "Functionalization, preparation and use of cell-laden gelatin methacryloyl–based hydrogels as modular tissue culture platforms," *Nature Protocols*, vol. 11, no. 4, pp. 727-746, 2016/04/01 2016, doi: 10.1038/nprot.2016.037.
- X. Ma et al., "Rapid 3D bioprinting of decellularized extracellular matrix with regionally varied mechanical properties and biomimetic microarchitecture," *Biomaterials*, vol. 185, pp. 310-321, 2018/12/01/ 2018, doi: <https://doi.org/10.1016/j.biomaterials.2018.09.026>.
- V. Magno, J. Friedrichs, H. M. Weber, M. C. Prewitz, M. V. Tsurkan, and C. Werner, "Macromolecular crowding for tailoring tissue-derived fibrillated matrices," *Acta Biomaterialia*, vol. 55, pp. 109-119, 2017/06/01/ 2017, doi: <https://doi.org/10.1016/j.actbio.2017.04.018>.
- A. Masamune, K. Kikuta, T. Watanabe, K. Satoh, M. Hirota, T. Shimosegawa, A. Masamune, and V. Bodempudi, "Hypoxia stimulates pancreatic stellate cells to induce fibrosis and angiogenesis in pancreatic cancer," *American Journal of Physiology-Gastrointestinal and Liver Physiology*, 01-Oct-2008. <https://doi.org/10.1152/ajpgi.90356.2008>
- A. Masamune, T. Watanabe, K. Kikuta, and T. Shimosegawa, "Roles of pancreatic stellate cells in pancreatic inflammation and fibrosis," (in eng), *Clin Gastroenterol Hepatol*, vol. 7, no. 11 Suppl, pp. S48-54, Nov 2009, doi: 10.1016/j.cgh.2009.07.038. ~
- B. N. Mason, A. Starchenko, R. M. Williams, L. J. Bonassar, and C. A. Reinhart-King, "Tuning three-dimensional collagen matrix stiffness independently of collagen concentration modulates endothelial cell behavior," (in eng), *Acta biomaterialia*, vol. 9, no. 1, pp. 4635-4644, 2013, doi: 10.1016/j.actbio.2012.08.007.

- E. Messineo, A. Pollins, and W. Thayer, "Optimization and evaluation of an in vitro model of PEG-mediated fusion of nerve cell bodies," *Journal of Clinical Neuroscience*, vol. 63, pp. 189-195, 2019/05/01/ 2019, doi: <https://doi.org/10.1016/j.jocn.2019.01.037>.
- A. C. Miklos, C. Li, N. G. Sharaf, and G. J. Pielak, "Volume Exclusion and Soft Interaction Effects on Protein Stability under Crowded Conditions," *Biochemistry*, vol. 49, no. 33, pp. 6984-6991, 2010/08/24 2010, doi: [10.1021/bi100727y](https://doi.org/10.1021/bi100727y).
- A. K. Miri et al., "Effective bioprinting resolution in tissue model fabrication," *Lab on a Chip*, vol. 19, 05/13 2019, doi: [10.1039/C8LC01037D](https://doi.org/10.1039/C8LC01037D).
- M. Nishimoto, K. Uranishi, M.N. Asaka, et al. Transformation of normal cells by aberrant activation of YAP via cMyc with TEAD. *Sci Rep*9, 10933 2019. <https://doi.org/10.1038/s41598-019-47301-6>
- F. Pati and D. W. Cho, "Bioprinting of 3D Tissue Models Using Decellularized Extracellular Matrix Bioink," (in eng), *Methods Mol Biol*, vol. 1612, pp. 381-390, 2017, doi: [10.1007/978-1-4939-7021-6_27](https://doi.org/10.1007/978-1-4939-7021-6_27).
- A. Porzionato, E. Stocco, S. Barbon, F. Grandi, V. Macchi, and R. De Caro, "Tissue-Engineered Grafts from Human Decellularized Extracellular Matrices: A Systematic Review and Future Perspectives," (in eng), *Int J Mol Sci*, vol. 19, no. 12, p. 4117, 2018, doi: [10.3390/ijms19124117](https://doi.org/10.3390/ijms19124117).
- T. J. Puls, X. Tan, C. F. Whittington, and S. L. Voytik-Harbin, "3D collagen fibrillar microstructure guides pancreatic cancer cell phenotype and serves as a critical design parameter for phenotypic models of EMT," (in eng), *PLoS One*, vol. 12, no. 11, p. e0188870, 2017, doi: [10.1371/journal.pone.0188870](https://doi.org/10.1371/journal.pone.0188870).
- T. Puls, X. Tan, M. Husain, C. Whittington, M. Fishel, and S. Voytik-Harbin, "Development of a Novel 3D Tumor-tissue Invasion Model for High-throughput, High-content Phenotypic Drug Screening," *Scientific Reports*, vol. 8, 12/01 2018, doi: [10.1038/s41598-018-31138-6](https://doi.org/10.1038/s41598-018-31138-6).
- T. Rajangam, M. H. Park, and S.-H. Kim, "3D Human Adipose-Derived Stem Cell Clusters as a Model for In Vitro Fibrosis," (in English), *Tissue Engineering Part C: Methods*, vol. 22, no. 7, pp. 679-690, Jul 2016, 2016-09-13 2016, doi: [http://dx.doi.org/10.1089/ten.tec.2016.0037](https://doi.org/10.1089/ten.tec.2016.0037).
- S. K. Ranamukhaarachchi et al., "Macromolecular crowding tunes 3D collagen architecture and cell morphogenesis," (in eng), *Biomater Sci*, vol. 7, no. 2, pp. 618-633, Jan 29 2019, doi: [10.1039/c8bm01188e](https://doi.org/10.1039/c8bm01188e).
- A. Ray, R. K. Morford, and P. P. Provenzano, "Cancer Stem Cell Migration in Three-Dimensional Aligned Collagen Matrices," (in eng), *Curr Protoc Stem Cell Biol*, vol. 46, no. 1, p. e57, Aug 2018, doi: [10.1002/cpsc.57](https://doi.org/10.1002/cpsc.57).

- A. J. Rice et al., "Matrix stiffness induces epithelial-mesenchymal transition and promotes chemoresistance in pancreatic cancer cells," (in eng), *Oncogenesis*, vol. 6, no. 7, p. e352, Jul 3 2017, doi: 10.1038/oncsis.2017.54.
- J. Rosenbloom, E. Macarak, S. Piera-Velazquez, and S. A. Jimenez, "Human Fibrotic Diseases: Current Challenges in Fibrosis Research," (in eng), *Methods Mol Biol*, vol. 1627, pp. 1-23, 2017, doi: 10.1007/978-1-4939-7113-8_1.
- A. Rubiano et al., "Viscoelastic properties of human pancreatic tumors and in vitro constructs to mimic mechanical properties," (in eng), *Acta Biomater*, vol. 67, pp. 331-340, Feb 2018, doi: 10.1016/j.actbio.2017.11.037.
- M. Sacchi, R. Bansal, and J. Rouwkema, "Bioengineered 3D Models to Recapitulate Tissue Fibrosis," *Trends in biotechnology*, Jun-2020. DOI: 10.1016/j.tibtech.2019.12.010
- S. D. Sackett et al., "Extracellular matrix scaffold and hydrogel derived from decellularized and delipidized human pancreas," (in eng), *Sci Rep*, vol. 8, no. 1, p. 10452, Jul 11 2018, doi: 10.1038/s41598-018-28857-1.
- G. A. Salg et al., "The emerging field of pancreatic tissue engineering: A systematic review and evidence map of scaffold materials and scaffolding techniques for insulin-secreting cells," (in eng), *J Tissue Eng*, vol. 10, p. 2041731419884708, Jan-Dec 2019, doi: 10.1177/2041731419884708.
- S. Samavedi and N. Joy, "3D printing for the development of in vitro cancer models," *Current Opinion in Biomedical Engineering*, vol. 2, pp. 35-42, 2017/06/01/ 2017, doi: <https://doi.org/10.1016/j.cobme.2017.06.003>.
- K. Shimizu, "Mechanisms of pancreatic fibrosis and applications to the treatment of chronic pancreatitis," (in eng), *J Gastroenterol*, vol. 43, no. 11, pp. 823-32, 2008, doi: 10.1007/s00535-008-2249-7.
- K. Shimizu, "Pancreatic stellate cells: Molecular mechanism of pancreatic fibrosis," *Journal of Gastroenterology and Hepatology*, vol. 23, no. s1, pp. S119-S121, 2008/03/01 2008, doi: 10.1111/j.1440-1746.2007.05296.x.
- Choi, Strauss, Robert, Richter, Maximilian, Yun, Lieber, and Andre, "Strategies to Increase Drug Penetration in Solid Tumors" *Frontiers*, 11-Jul-2013. doi: 10.3389/fonc.2013.00193
- T. Sun, X. Li, Q. Shi, H. Wang, Q. Huang, and T. Fukuda, "Microfluidic Spun Alginate Hydrogel Microfibers and Their Application in Tissue Engineering," (in eng), *Gels*, vol. 4, no. 2, p. 38, 2018, doi: 10.3390/gels4020038.
- K. E. Sung et al., "Control of 3-dimensional collagen matrix polymerization for reproducible human mammary fibroblast cell culture in microfluidic devices," *Biomaterials*, vol. 30, no. 27, pp. 4833-4841, 2009/09/01/ 2009, doi: <https://doi.org/10.1016/j.biomaterials.2009.05.043>.

- V. Thomas, M. V. Jose, S. Chowdhury, J. F. Sullivan, D. R. Dean, and Y. K. Vohra, "Mechano-morphological studies of aligned nanofibrous scaffolds of polycaprolactone fabricated by electrospinning," (in eng), *J Biomater Sci Polym Ed*, vol. 17, no. 9, pp. 969-84, 2006, doi: 10.1163/156856206778366022.
- F. Watt, W. Huck, "Role of the extracellular matrix in regulating stem cell fate" *Nat Rev Mol Cell Biol* 14, 467–473 2013. <https://doi.org/10.1038/nrm3620>
- C. J. Whatcott, R. G. Posner, D. D. Von Hoff, and H. Han, "Desmoplasia and chemoresistance in pancreatic cancer," in *Pancreatic Cancer and Tumor Microenvironment*, P. J. Grippo and H. G. Munshi Eds. Trivandrum (India): Transworld Research Network Transworld Research Network., 2012.
- M. Wurm et al., "in vitro evaluation of Polylactic acid (PLA) manufactured by fused deposition modeling," *Journal of Biological Engineering*, vol. 11, p. 29, 12/01 2017, doi: 10.1186/s13036-017-0073-4.
- T. A. Wynn, "Cellular and molecular mechanisms of fibrosis," (in eng), *J Pathol*, vol. 214, no. 2, pp. 199-210, Jan 2008, doi: 10.1002/path.2277.
- F. Xu, I. Gough, J. Dorogin, H. Sheardown, and T. Hoare, "Nanostructured degradable macroporous hydrogel scaffolds with controllable internal morphologies via reactive electrospinning," *Acta Biomaterialia*, vol. 104, pp. 135-146, 2020/03/01/ 2020, doi: <https://doi.org/10.1016/j.actbio.2019.12.038>.
- K. Xu et al., "3D porous chitosan-alginate scaffold stiffness promotes differential responses in prostate cancer cell lines," *Biomaterials*, vol. 217, p. 119311, 2019/10/01/ 2019, doi: <https://doi.org/10.1016/j.biomaterials.2019.119311>.
- M. Xu, X. Wang, Y. Yan, R. Yao, and Y. Ge, "An cell-assembly derived physiological 3D model of the metabolic syndrome, based on adipose-derived stromal cells and a gelatin/alginate/fibrinogen matrix," (in eng), *Biomaterials*, vol. 31, no. 14, pp. 3868-77, May 2010, doi: 10.1016/j.biomaterials.2010.01.111.
- A. S. Zeiger, F. C. Loe, R. Li, M. Raghunath, and K. J. Van Vliet, "Macromolecular Crowding Directs Extracellular Matrix Organization and Mesenchymal Stem Cell Behavior," *PLOS ONE*, vol. 7, no. 5, p. e37904, 2012, doi: 10.1371/journal.pone.0037904.
- C. Zeltz, I. Primac, P. Erusappan, J. Alam, A. Noel, and D. Gullberg, "Cancer-associated fibroblasts in desmoplastic tumors: emerging role of integrins" *Seminars in Cancer Biology*, 12-Aug-2019. doi: 10.1016/j.semcancer.2019.08.004. doi: 10.1016/j.semcancer.2019.08.00
- H. X. Zhou, "Effect of mixed macromolecular crowding agents on protein folding," (in eng), *Proteins*, vol. 72, no. 4, pp. 1109-13, Sep 2008, doi: 10.1002/prot.22111.

Appendices

Appendix A: USDA Guidelines

Examination of animals prior to slaughter; use of humane methods

- (a) Examination of animals before slaughtering; diseased animals slaughtered separately and carcasses examined

For the purpose of preventing the use in commerce of meat and meat food products which are adulterated, the Secretary shall cause to be made, by inspectors appointed for that purpose, an examination and inspection of all amenable species before they shall be allowed to enter into any slaughtering, packing, meat-canning, rendering, or similar establishment, in which they are to be slaughtered and the meat and meat food products thereof are to be used in commerce; and all amenable species found on such inspection to show symptoms of disease shall be set apart and slaughtered separately from all other cattle, sheep, swine, goats, horses, mules, or other equines, and when so slaughtered the carcasses of said cattle, sheep, swine, goats, horses, mules, or other equines shall be subject to a careful examination and inspection, all as provided by the rules and regulations to be prescribed by the Secretary, as provided for in this subchapter.

- (b) Humane methods of slaughter

For the purpose of preventing the inhumane slaughtering of livestock, the Secretary shall cause to be made, by inspectors appointed for that purpose, an examination and inspection of the method by which amenable species are slaughtered and handled in connection with slaughter in the slaughtering establishments inspected under this chapter. The Secretary may refuse to provide inspection to a new slaughtering establishment or may cause inspection to be

temporarily suspended at a slaughtering establishment if the Secretary finds that any cattle, sheep, swine, goats, horses, mules, or other equines have been slaughtered or handled in connection with slaughter at such establishment by any method not in accordance with the Act of August 27, 1958 (72 Stat. 862; 7 U.S.C. 1901–1906) until the establishment furnishes assurances satisfactory to the Secretary that all slaughtering and handling in connection with slaughter of livestock shall be in accordance with such a method.

Sanitary inspection and regulation of slaughtering and packing establishments; rejection of adulterated meat or meat food products

The Secretary shall cause to be made, by experts in sanitation or by other competent inspectors, such inspection of all slaughtering, meat canning, salting, packing, rendering, or similar establishments in which amenable species are slaughtered and the meat and meat food products thereof are prepared for commerce as may be necessary to inform himself concerning the sanitary conditions of the same, and to prescribe the rules and regulations of sanitation under which such establishments shall be maintained; and where the sanitary conditions of any such establishment are such that the meat or meat food products are rendered adulterated, he shall refuse to allow said meat or meat food products to be labeled, marked, stamped or tagged as "inspected and passed."

Appendix B: Extracellular Matrix Extraction Protocol

Materials:

- Pig pancreas
- 1X PBS
- 10X PBS
- Distilled water
- Centrifuge
- Sieve
- HCl solution
- Sodium deoxycholate (Sigma Aldrich, D6750-10G)
- Pepsin solution (Sigma Aldrich, P7012-1G)
- 40 μ m filter
- NaOH
- 24 well culture plate
- Conical tubes (varying volumes)
- Beakers (varying volumes)
- Scalpels
- Homogenizer
- Lyophilizer
- Shaker

Method:

Pancreas Decellularization

1. The pancreas will be trimmed of surrounding fat.
2. The pancreas will be sectioned into 1cm³ pieces.
3. Rinsed with 1x PBS for 30mins.
4. Wash the pieces with distilled water.
5. Homogenize in distilled water until pancreas tissue is broken up
6. Centrifuge for 5 mins @ 4300 RPM

7. Remove any fat floating on the surface
8. Discard supernatant.
9. Resuspend the pellet and repeat steps 6-8.
10. Discard supernatant and resuspend the pellet in 2.5mM sodium deoxycholate/PBS and incubate for 3 hours at room temperature on a shaker.
11. Strained the homogenate over a sieve
12. All collected material placed back in 2.5mM sodium deoxycholate/PBS for 15 hours at room temperature on a shaker.
13. Strained the material again over a sieve and rinsed with distilled water
14. Wash the material with 1X PBS and pen/strip for 72 hours at room temperature on a shaker, rinsing with water and changing PBS and pen/strip daily.
15. Repeat step 14 w/ distilled water
16. Snap freeze and powderize in mortar and pestle before lyophilization
17. Lyophilize and store the material in -80°C for future use.

Hydrogels Formation

1. ECM should be digested with an HCl/pepsin solution
2. 1g powder:100mg pepsin are mixed in 100ml of 0.01M of HCl, keeping constant stirring for approximately 48 hours at room temperature.
3. Mixing solution with 0.1 N NaOH (1/10 volume of solution) and 10X PBS pH 7.4 (1/9 volume of solution) in 4°C .
4. Add cold (4°C) 1x PBS pH 7.4 to desired volume/concentration and bring to 37°C for

gelation.

Hydrogel Coated Plates

1. Acidic ECM digest was diluted with cold 1X PBS to a concentration of 0.08 mg/ml (a 1:120 dilution)
2. Filtered through a 40 μ m filter to remove undigested ECM pieces
3. 300 μ l of diluted digest (pre-gel solution) was added to each well of a chilled 24-well culture plate
4. Plates were incubated at 37 °C for one hour and rinsed with PBS before use.

Appendix C: Protocol for Collagen Hydrogel with Single Crowders

Materials:

- Ice container and ice
- 1X PBS
- Distilled water
- Collagen type I
- 96 well plate
- 70% ethanol
- Positive displacement pipettes/tip
- Pipettes/tips
- Microtubes
- Neutralization solution
- PEG (8kDa) solution
- Ficoll 70 solution
- Ficoll 400 solution
- Sharpie

Methods

Collagen Protocol

1. Retrieve ice bucket, and fill with ice
 - a. Place collagen type I, neutralization solution, crowding agent solutions, and 1X PBS on ice to prevent spontaneous polymerization.
2. Work in a sterile environment, and spray everything with 70% ethanol
3. Determine number of groups, replications, and volume per well for collagen type I
 - a. Number of groups = _____
 - b. Number of replications = _____
 - c. Volume per well = _____
 - d. Final Volume = # groups * # replications * Volume per well = _____
4. Determine initial concentration, and final concentration for collagen
 - a. Initial concentration of collagen type I = _____

- i. Notes: For collagen, account for concentration after neutralization as well
 - ii. Initial concentration * 0.9 = _____
 - b. Desired final concentration of collagen type I = _____
 - c. Using $C_1V_1 = C_2V_2$ to determine initial volume of collagen I
 - i. $V_1 = (4b*3d)/4a = \text{_____} * 1.1$
 - 1. Notes: Due to how thick collagen is, there is lost so always make more than needed.
- 5.** Repeat step 3 & 4 for each crowding agent condition
- a. Notes: number of groups will be 1.
 - b. Determine number of conditions per crowding agent
 - c. Add volume found in 4c for each condition per crowding agent to obtain total volume for each crowding agent solution.
- 6.** Label microtubes for each condition and keep on ice.
- 7.** Determine volume of stock from collagen type I, crowding agent solution, and PBS to add to each microtube. Use $C_1V_1 = C_2V_2$.
- a. Total volume from collagen stock = $(3b*3c*4b)/4aii$
 - b. Total volume from crowding stock = $(3b*3c*4b)/4a$
 - c. Total volume to dilute with 1X PBS = $(3b*3c) - (7a+7b)$
- 8.** Mix solutions in 2mL microtubes well.
- 9.** Pipette (3c) of each microtube in wells x(3b)
- a. Remember to always have a control group.
 - b. Be sure to label, date, and initial

10. Place the 96 well plate in the incubator at 37°C until gel.
11. Add 50uL of 1X PBS to each well with groups to prevent drying
12. Wrap 96 well plates with parafilm and store in 4°C until ready to image.
 - a. Notes (Figure 14) is an example of how to set up the 96 well plates

































































































Crowders		1 mg/mL	3 mg/mL	6 mg/mL	C								
		1	2	3	4	5	6	7	8	9	10	11	12
Ficoll 70	A												
Ficoll 400	B												
PEG	C												
	D												
	E												
	F												
	G												
	H												

Figure 14: Schematic of well plates set up with 1 mg/mL of collagen. C stands for control with no crowding agents. Ficoll 70 is in row B, Ficoll 400 is in row D, PEG is in row F. Concentrations were placed as follows: 1 mg/mL (2-4), 3 mg/mL (5-7), 6 mg/mL (8-10).

Appendix D: MMC Confocal Imaging and Analysis

Materials:

- 1 x PBS
- 1 x Glass-bottom Petri Dish

Programs:

FIJI ImageJ

Methods:

MMC Confocal Microscopy Protocol (Leica Point Scanning Confocal SP5)

1. Gels are placed on a glass-bottom Petri dish.
2. Add 1 x PBS to the Petri dish preventing the gel from drying out.
3. Ensure the microscope is using the 20x objective lens
4. Apply immersion oil to 20x lens
5. If Collagen is not stained, reflectance mode must be turned on
6. Capture and label pictures as needed
7. Export images as either .TIFF or .JPEG for analysis via ImageJ (.TIFF is preferred over .JPEG due to no loss of image resolution)

Directionality analysis of image Protocol

1. Load the image of interest in ImageJ
2. Select “image” → “type” → “8-bit”.

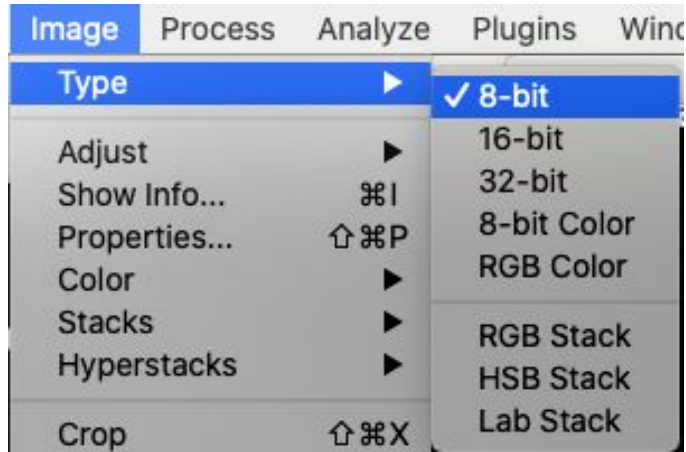


Figure 15: Menu location of “8-bit” tab

3. Run the directionality plugin,
 - a. Select “Analyze” → “directionality”.

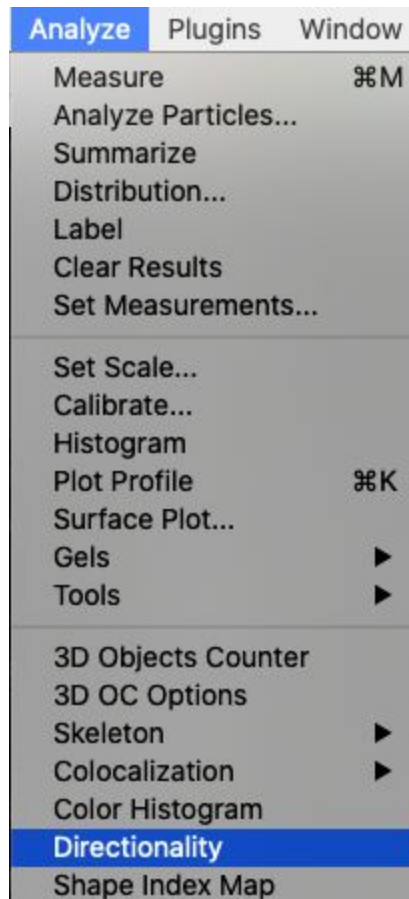


Figure 16: Menu location for “Directionality” tab

Pore size and Pore Number Protocol

1. Load the image being analyzed
2. Select “image” → “type” → “8-bit”

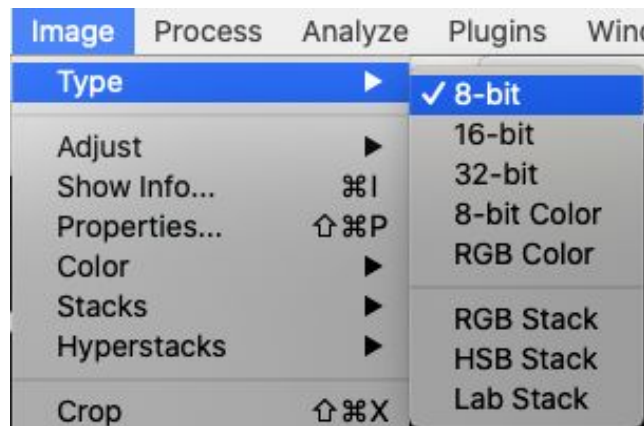


Figure 17: Menu path for selecting “8-bit”

3. Set the correct scale bar (If the original scale bar is correct in length and unit, there's no need to reset it.)
 - a. Select “analyze” → “set scale” → “remove existing scale”, then add the correct scale.

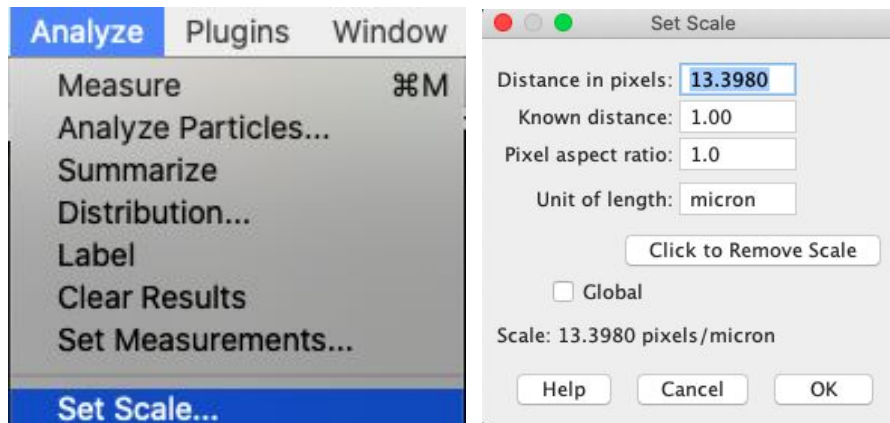


Figure 18: Menu path for locating “Set scale” and “Remove scale”

4. Set Fast Fourier Transform (FFT) bandpass filter

- a. Select “process” → “FFT” → “bandpass filter”

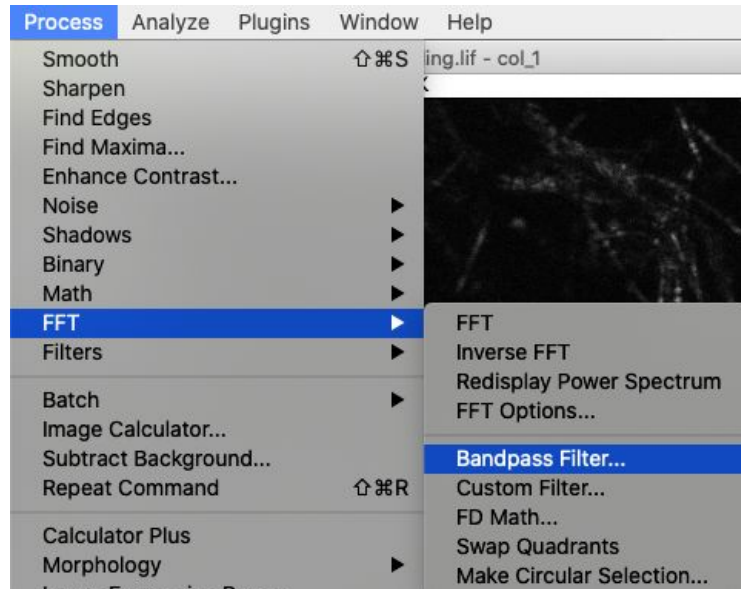


Figure 19: Menu path for “Bandpass Filter”

5. Set the threshold

- a. Select “image” → “adjust” → “auto threshold”

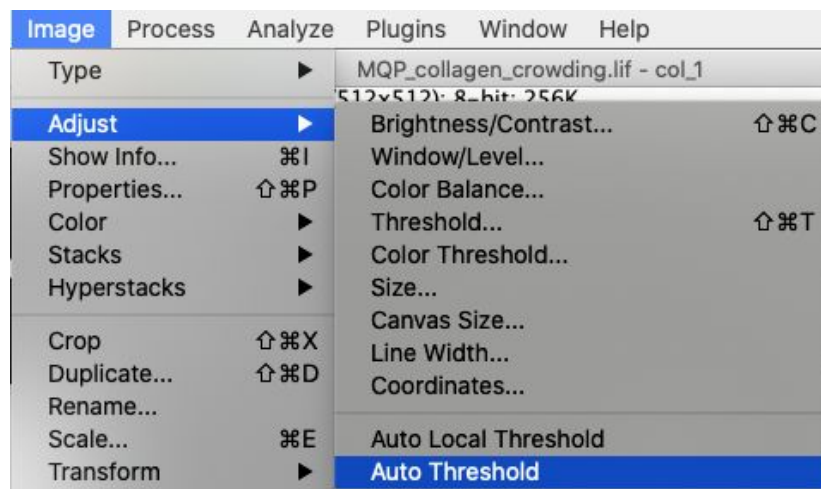


Figure 20: Menu path for selecting “Auto Threshold”

6. Select and duplicate the desired image.

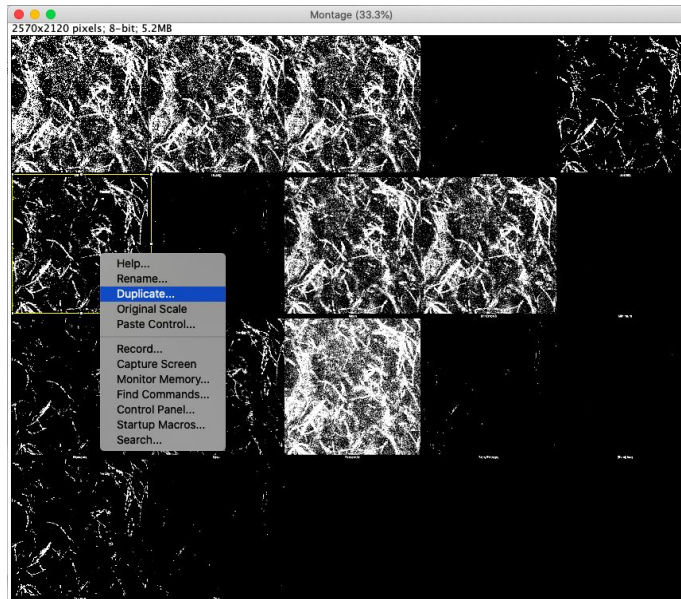


Figure 21: Selecting and duplicating an image

7. Select the “image” tab → “adjust” → “threshold” on the new image and drag the bottom bar all the way to the right and click “apply” for porosity.

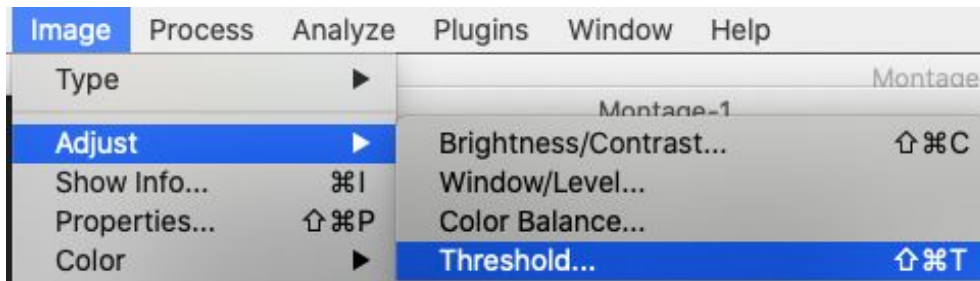


Figure 22: Menu path for “Threshold”

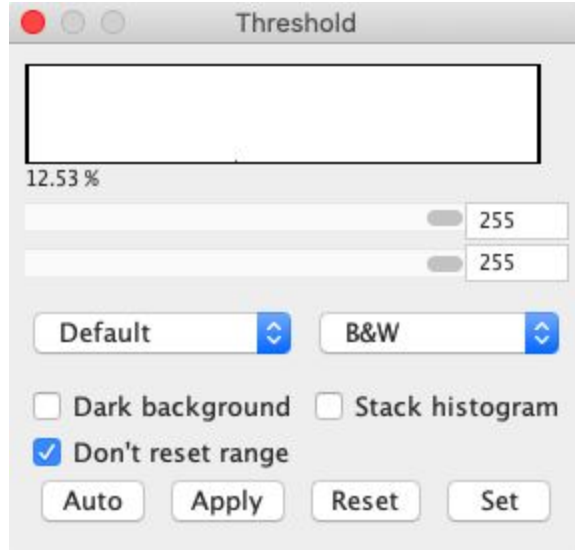


Figure 23: Setting for Porosity in Threshold

8. Select “analyze” → “analyze particles” → “display clear results”

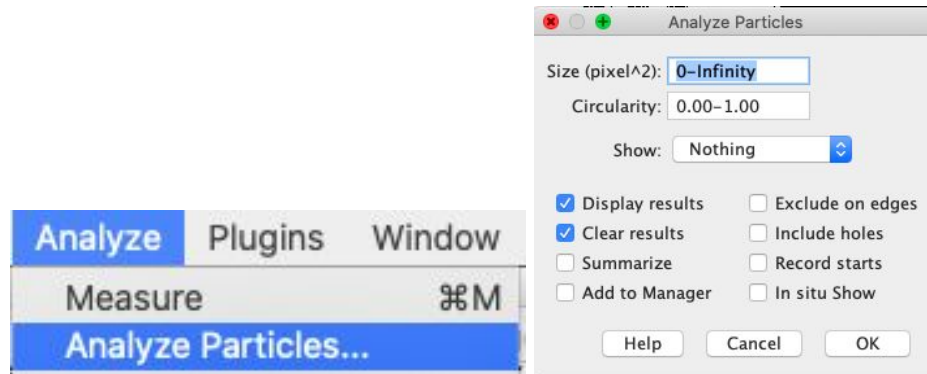


Figure 24: Menu path for selecting “Analyze Particles” and “Display Result”

9. A list of results will be generated which represents the areas of porosity. Use the following equation to calculate the radii from the list of areas :

$$R = \sqrt{(area)/\pi}$$

Appendix E: Electrospinning protocol

Electrospun Parameters to Adjust

1. Change the distance between the needle and the collection mesh. (4in, 8in, 12in)
2. Change the concentration of the solution. (1 mg/ml, 3mg/ml, 6mg/ml)
3. Adjust the voltage as needed to create a cone at the tip of the needle.
4. Adjust the rate the solution is being electrospun (0.5 ml/hr, 1 ml/hr, 2 ml/hr)
5. Experimental groups

Table 11: Fixed and changing parameter of electrospinning.

Agents	Size	Voltage	Rate	Concentration	Distance
Pancreatic ECM	21G	Adjust	Adjust	5.2mg/ml	4inches
				3mg/ml	8inches
				1mg/ml	12 inches
PEO/Alginate	21G	Adjust	Adjust	0mg/mL	4in
				12mg/mL	8in
				20mg/mL	12in
				28mg/mL	
				40mg/mL	
Collagen	21G	Adjust	Adjust	5.2mg/ml	4in
				3mg/ml	8in
				1mg/ml	12in

Electrospinning Protocol

Materials:

- Agents
- Syringe pump
- 5mL syringe
- 21G blunt needle
- Voltage source
- Collection mesh (tin foil)
- Polycarbonate containment area

Procedure

1. Make solution of Agent
2. Set up electrospinning equipment
 - a. Mount syringe in syringe pump. Set syringe diameter to 12.6mm (for 5ml syringes) and the flow rate.
 - b. Ground setup by attaching the yellow alligator clip to a piece of foil (the collection mesh)
 - c. Attach the green alligator clip to the tip of the syringe needle
 - d. Position syringe needle tip to desire distance
3. Close the door to the polycarbonate containment area

4. When you start to see a small amount of solution just coming out of the syringe, turn on the voltage. Adjust the voltage to see the material make a cone shape as it sprays in the direction of the collection mesh.
 - a. Too low will cause solution to drip
 - b. Too high will cause the solution to spray all over area
 - c. Never work in the containment area while voltage is on.
5. When finished, turn off the voltage, then the syringe pump.